

PAPER

View Article Online
View Journal | View Issue



Cite this: *Environ. Sci.: Processes Impacts*, 2020, 22, 1266

Sorption of surfactants onto sediment at environmentally relevant concentrations: independent-mode as unifying concept†

Hildo Krop, ^{*a} Pim de Voogt, ^{*bc} Christian Eschauzier^d and Steven Droge ^b

At low surfactant concentrations often non-linear sorption processes are observed when natural adsorbents like sediment or soil are involved. This sorption process is often explained by a Dual-Model (DM) model, which assumes sorption to an adsorbent to be based on a combined ionic-polar and non-polar sorption interaction term. An Independent-Mode (IM) model, however, could treat surfactant sorption as two independent sorption processes to which the non-polar and ionic-polar features of the surfactant molecule contribute differently. For both models the overall exact partition coefficient, K_p^{total} , and its corresponding total standard free enthalpy of adsorption, $\Delta_s G_{\text{total}}^0$, are derived. We tested the outcome of both models against multiple published experimental sorption data sets by, (i) varying the organic carbon fraction, (ii) constructing sorption and partition isotherms over different concentration ranges, (iii) removing the organic carbon fraction, (iv) applying different types of mixtures of surfactants, and (v) explaining sorption hysteresis in desorption studies based on either continuous and successive washing steps. It turned out that only the IM model was able to explain the reported sorption phenomena. We also show that when one interaction is dominating, e.g. non-polar over ionic-polar, the $\Delta_s G_{\text{total}}^0$ of the IM model can be approximated by the sum of the different $\Delta_s G^0$ values, the $\Delta_s G_{\text{total}}^0$ of the DM model. The exact partition coefficient, $K_p(C_w)$ (L kg^{-1}) = dC_s (mmol kg^{-1})/ dC_w (mmol L^{-1}), is turning each sorption isotherm into a partition isotherm that provides the K_p values required in environmental risk assessment models.

Received 11th December 2019
Accepted 3rd March 2020

DOI: 10.1039/c9em00580c

rsc.li/espi

Environmental significance

This paper addresses ad- and desorption processes of surfactants at environmentally low concentrations onto sediments. Reported models show that both the head and tail of the same surfactant molecule is involved in a single sorption process (Dual-Mode). This paper shows that all experimentally observed sorption phenomena can be explained by sorption of the tail of one surfactant molecule to one location while the head of another surfactant molecule will be adsorbed to another sorption location (Independent-Mode). The study emphasizes that only complete Langmuir isotherms are able to explain adequately many observed sorption phenomena. In applying the Independent-Mode model we define an exact K_p function. In sorption experiments of surfactants on complex adsorbents one requires to define the relevant adsorbents and apply for each fraction simple Langmuir isotherms. In ERA models one needs to estimate two sorption parameters for each relevant adsorbent.

1. Introduction

The sorption behaviour of chemicals in the environment is characterized by the ratio of the concentration of the substance

associated with water, C_w (mg L^{-1} or mmol L^{-1}), and the amount of substance associated with a volume of a sorbent such as sediment, C_s (mg kg^{-1} or mmol kg^{-1}). At equilibrium, this ratio is equivalent to the sediment–water partition coefficient, K_p (L kg^{-1}), eqn (1):

$$K_p = C_s/C_w \quad (1)$$

The K_p plays an important role in environmental fate models and in environmental risk assessment (ERA). For example it is required to estimate the bioavailable fraction of the sorbate in different environmental compartments. In ERA models sorption of organic substances is currently addressed only via a hydrophobic or non-polar interaction mechanism. In these models sorption is incorporated as a linear process. It is also

^aKrop-Consult, Conradstraat 7, 1505KA Zaandam, The Netherlands. E-mail: h.b.krop@uva.nl; Tel: +31 614988669

^bUniversity of Amsterdam (UvA), Institute for Biodiversity and Ecosystem Dynamics (IBED), Science Park 904, 1098 XH Amsterdam, The Netherlands

^cKWR Water Research Institute, Groningenhaven 7, 3433 PE Nieuwegein, The Netherlands

^dEschauzier Water Management, Trouwringhstraat 18-1, 1055HB Amsterdam, The Netherlands

† Electronic supplementary information (ESI) available. See DOI: 10.1039/c9em00580c



generally found that the hydrophobic or non-polar sorption increases proportionally with increasing organic carbon fraction (f_{oc}) of the sorbent, making it logical to normalise the sediment–water partition constant, K_p , to the organic carbon fraction, K_{oc} . These K_{oc} values are used as dependent descriptor for structure–activity relationships (SARs) *e.g.* with the octanol–water partition coefficient, K_{ow} , as independent descriptor.

Surface-active agents (surfactants) are molecules consisting of an ionic, polar, or otherwise hydrophilic head and a hydrophobic (lipophilic) tail. Because of their amphiphilic character their sorption behaviour is different from purely hydrophobic compounds and may also include an electrostatic or ionic–polar sorption process. These sorption processes are described clearly in colloid chemistry. On pure surfaces like silica, kaolinite, or montmorillonite over a large concentration range the sorption process of many surfactants is characterised by a distinct four steps adsorption pattern.^{1–3} At low concentrations sorption is linear and the sorption process is only restricted to an exchange process between isolated molecules and the surface referred to as the Henry's law region. At higher concentrations surfactant molecules start to form micellar-like structures on the surface commonly denoted as admicelles and hemicelles followed by the formation and sorption of micelles. Unless waste waters enter aquatic systems without any treatment, surfactant concentrations encountered in the environment are in general so low, *i.e.* in the order of $\mu\text{g L}^{-1}$ or lower, that micellar-like structures are not expected.^{4,5} However, even if an ionic–polar sorption process is expected to occur at a sorbent within the Henry's law region it is observed that the sediment–water partition coefficient increases with increasing carbon chain length of analogue surfactants (*i.e.* increasing number of CH_2 or CF_2 -units).^{6–9} In environmental and colloid chemistry this is generally interpreted as an additional or non-polar sorption interaction of the tail with the sorbate.^{10,11} In these models both the head and the tail of the surfactant molecule are involved simultaneously in an adsorption process. In the present work this is called the Dual-Mode (DM) adsorption process because only one type of adsorbent is involved, as depicted in Fig. 1a. The DM models lead to a picture that the surfactant molecules should be (partially) absorbed into the matrix, requiring the

introduction in the model of parameters that are related to the structure of the matrix.

To our best knowledge, it has not been described well in the scientific sorption literature what sorption isotherm would be obtained if sorption of surfactants to adsorbents is described by an Independent-Mode (IM) adsorption process, as an alternative to the DM model. In the IM model one surfactant molecule (or one part of the total adsorbed mass of the surfactant) is adsorbed by a non-polar mechanism to an organic-carbon like sediment component, and another surfactant molecule (or, the other part of the total adsorbed mass) is adsorbed (only) by an ionic–polar mechanism to another sediment component (*e.g.* clay mineral surface), as depicted in Fig. 1b.

Although Fig. 1 is overly simplistic, intuitively it makes sense that the description of these two models could lead to different conclusions on how surfactant sorption can be best described. A correct interpretation of observed sorption phenomena for surfactants is of importance for risk assessment modelling of potential contamination with such chemicals. Regulators may have to extrapolate results from the experimental boundaries to specific case studies with different features, sorbent properties, and concentration ranges. As outlined below in more detail the goal of this study was two-fold. In the theoretical considerations we derive the relevant thermodynamic equations for the standard free enthalpy change, $\Delta_s G_{\text{total}}^0$, of the sorption process for both the DM and IM model. For both models, the overall adsorption isotherm (K_p^{total}) which combines both types of interactions between surfactant and the sorbent surface (non-polar and polar-ionic) is then derived. These mathematical descriptions should elucidate how the relevant partition coefficients can be derived to support environmental risk assessment for surfactants. In the model application section we evaluated outcomes of both models against multiple published experimental sorption data sets involving various sorption phenomena. By simulating the variations of several sorption parameters differences between IM and DM sorption isotherms are interpreted and compared with observed isotherms. We will show that interpretation of these differences shows full support for the IM model. The DM model is used in the development of sorption models based on thermodynamics but we will show that the same results are found using the IM model when one of the two interaction modes dominates.

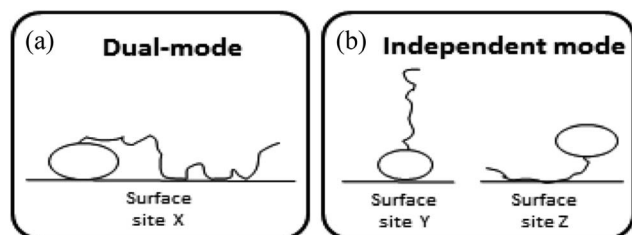


Fig. 1 Schematic representation of the difference in sorption of surfactant molecules to adsorbents. In the DM model (a) both the head and the tail of the surfactant molecule are adsorbed simultaneously to one adsorbent only. In the IM model (b) the head of one surfactant molecule is electrostatically adsorbed to a specific adsorbent or sorption location while the tail of another surfactant molecule is adsorbed to a another sorption location or adsorbent.

2. Theoretical considerations

2.1 Introduction

In this paper it is assumed that in the environment sediment–water and/or soil/water adsorption processes are dominant particularly for the fate of surfactants. Therefore soil/air adsorption processes are excluded in the present study. In environmental chemistry one refers often to hydrophobic *vs.* electrostatic adsorption processes when dealing with especially ionic surfactants. This excludes the possibility for an electrostatic attraction of the non-ionic but highly polar head, like *e.g.*, for non-ionic surfactants such as alcohol ethoxylates (AE) to sediment or soil. To include the possibility of different types of electrostatic interactions for various surfactants, we refer in the



text to an *ionic-polar* adsorption process when the head of any surfactant is involved in the adsorption process, but in the relevant mathematical formulas we keep on using the abbreviation 'elec'. Similarly, the hydrophobic adsorption processes of the tail of a surfactant is described in the text as a *non-polar* adsorption process, but we keep the abbreviation 'hydr' in the mathematical formulas. These abbreviations align with the mathematics of sorption models applied elsewhere.

Absorption into some sorbents may also occur for surfactants, but these processes are also not within the subject of the present study on sorption to soil or sediment. It has been reported that ionic surfactants fully intercalate within phospholipid membranes.^{12,13} Also the solid-phase microextraction process for non-ionic surfactants such as AE with polyacrylate coated glass fibers appears to be based on absorption of the entire surfactant molecules into the rubbery polymer matrix.^{14,15}

By far most sorption experiments of surfactants performed in the laboratory apply a short time span where aging phenomena are neglected. When applying aging processes fast and slow (into micropores of sediment or soil) ad- or desorption fractions may be observed^{16,17} but in this paper it will be shown that the IM model can explain such phenomena for surfactants without invoking additional adsorption into micropores (for a more fundamental discussion on the different ranges of validity of especially the kinetic Langmuir sorption-diffusion model see for example the work of Douven *et al.*¹⁸). All applied literature references to test our developed model are performed in a relatively short time span (hours to days).

At low concentrations (usually, but not specifically, at the $\mu\text{g L}^{-1}$ level) both non-linear and linear sorption of surfactants to pure and complex adsorbents are observed.¹⁹ The observed non-linear sorption processes are often described by a Langmuir, Freundlich, or Virial isotherm. Also more complex models like combinations of a linear and one or more Langmuir, Temkin, Toth isotherms or the non-ideal competitive adsorption (NICA)-Donnan model have been proposed.^{20–24} The models establish a relationship between a number of data points of measured concentrations C_s in soil or sediment and concentrations C_w in water, at equilibrium. In the present work we refer to the ratios of such measured data, obtained from the applied experimental system, as partition coefficients, K_p (L kg^{-1}). The partition coefficients thus derived need to be linked to the molecular adsorption system to develop sorption models and/or SARs. Parameters related to molecular adsorption processes are called sorption constants, K (unit *e.g.* L mmol^{-1}). In thermodynamical terms we have to distinguish two different systems here. In order to relate K_p to K , a change in (thermodynamic) system is therefore involved; from the experimental one to the molecular one. In the experimental system certain parameters, *e.g.*, temperature or pH, are often modified to establish the variation of the partition coefficient. We show that one needs to be careful to interpret measured variation in K_p as a result of *e.g.*, varying pH values into variations in (molecular) sorption constants, K .

From the different non-linear models the most simple one to interpret is the Langmuir model. In this case the non-linearity is caused by the limited number of sorption sites in the applied experimental system. At low concentrations where no

micellization occurs it is therefore assumed that the observed non-linearity is a consequence of the availability of a limited number of sorption sites in the applied experimental system. Before any molecular adsorption process can be studied this non-linear adsorption strength in the applied experimental system must be accounted for. This is done by studying the sorption behaviour at infinite dilution. This behaviour is not only important to establish molecular sorption models but environmentally very relevant since it coincides with a dilution process. K_p values corrected for their non-linear behaviour at infinite dilution are indicated as $K_{p,0}$. Only $K_{p,0}$ -values lead therefore to relevant information on the molecular sorption process(es).

The relevant sorption parameters for the IM and DM models will be derived in a stepwise approach. The first step describes the behaviour of the most common isotherms at infinite dilution to account for the limited number of sorption sites in the applied experimental system.

Non-linear sorption isotherms imply that the corresponding K_p depends on the dissolved concentration of the compound (C_w), $K_p(C_w)$. In the second step it will be shown how the $K_p(C_w)$ can be derived from any (non-linear) isotherm by defining an 'exact' partition coefficient, K_p . It will be shown that the partition coefficient from eqn (1) is an 'average' K_p , $\bar{K}_p(C_w)$.

In the third step the relevant thermodynamic equations will be derived for the standard free enthalpy change, $\Delta_s G_{\text{total}}^0$, of the sorption process and for the overall partition coefficient, K_p^{total} , which encompasses both the non-polar and ionic-polar interactions for both the IM and DM model. Finally the step from the experimentally derived parameter, $K_{p,0}$, to the molecular sorption constants will be discussed. In this part also attention will be given to observed rate phenomena of any adsorption or desorption process for surfactants.

2.2 Behaviour of commonly used sorption isotherms at infinite solution ($C_s, C_w \rightarrow 0$)

2.2.1 Langmuir sorption isotherm. The Langmuir case I isotherm²⁵ applied to solutions relates the adsorption of a specific solute (or adsorbate) to a fixed number of unique distinct sites or a maximum of mass adsorbed to the adsorbent, C_s^{max} (mg or mmol substance per kg sediment), each site, S , being occupied by one single solute molecule, M , only. In equilibrium, the number of unoccupied, S^* , and occupied sorption sites, $S-M$, and the solute concentration M_{aq} ($S^* + M_{\text{aq}} \xrightleftharpoons[k_a]{k_d} S-M$) are related to each other by the Langmuir case I sorption constant, K_L (L mg^{-1} or mmol^{-1}) and is also equal to the ratio of the adsorption and desorption rate constants, k_a/k_d . The fraction of surface sites occupied, $S-M/(S^* + S-M)$, C_s/C_s^{max} , can be written in the operational way *cf.* eqn (2):

$$\frac{C_s}{C_s^{\text{max}}} = \frac{K_L C_w}{1 + K_L C_w} \quad (2)$$

In dilute solutions (more accurate when $K_L C_w \ll 1$) eqn (2) can be rewritten as eqn (3) where a Langmuir sediment-partition coefficient, K_p^L , can be derived that is not influenced



any more by the number of unoccupied sites, $K_{p,0}^L$ ($L\text{ kg}^{-1}$),^{26,27} (eqn (3a) and (3b)):

$$C_{s \rightarrow 0} = K_L C_s^{\max} C_{w \rightarrow 0} \quad (3a)$$

$$\frac{C_{s \rightarrow 0}}{C_{w \rightarrow 0}} = K_L C_s^{\max} = K_{p,0}^L \quad (3b)$$

Using eqn (3b), eqn (2) can then be rewritten into the (thermodynamic) expression of $K_{p,0}^L$ as follows, eqn (4), used throughout in this study.

$$C_s = \frac{K_{p,0}^L C_s^{\max} C_w}{C_s^{\max} + K_{p,0}^L C_w} \quad (4)$$

Reported C_s and C_w values and isotherms are usually normalised to 1 kg of sediment and 1 L of water respectively. In Annex I it is shown that eqn (4) arises from a general Langmuir sorption process, which includes the sediment concentration while neglecting the sediment volume.

It is important to realize that eqn (4) can become linear both at infinite dilution, as described above, and when $C_s^{\max} \gg K_{p,0}^L C_w$ (that is for low fraction of surfactant adsorbed in relation to a high number of sorption sites). Therefore it is assumed in this study that whenever a linear isotherm at low surfactants concentrations is observed this is not only a consequence of the Langmuir isotherm at infinite dilution but it is also equivalent to the Henry's law isotherm observed at low surfactant concentrations on pure adsorbents. The IM model therefore supposes that an observed linearity in sorption at low concentrations is a general consequence of a Langmuir isotherm where the number of occupied sorption sites in the applied experimental system is still low compared to the total number of sorption sites.

On the other hand, any observed non-linear behaviour of the Langmuir case I isotherm at higher surfactant concentrations is a consequence of a preference of one of two different processes: either C_s^{\max} is approached and the curvature will decrease until a plateau, C_s^{\max} , is reached or the curvature will increase before C_s^{\max} is approached which is related to the formation of admicelles, hemicelles or possible multiple layers²⁸ on the adsorbent (neglecting for example additional chemical processes like an exchange of ligands from the adsorbent). Since at environmental concentrations micelle structures are not expected only decreasing curvature is expected for single Langmuir isotherms. In the discussion attention will be given when to be aware of possible micellization at higher surfactant concentrations.

2.2.2 Henry's law isotherm. Sorption isotherms described by a simple linear equation are Henry's law isotherms: $C_s = K_p^H C_w$. Owing to its linearity K_p^H does not change when diluting ($K_p^H = K_{p,0}^H$). As described above the observed Henry's law isotherm of the non-polar interaction with partition coefficient, $K_p^{H,hydr}$, derived from the K_{oc} of the substance and the fraction of organic carbon of the sediment, f_{oc} , can be related to the linear form of the Langmuir isotherm (see Section 2.2.1) at infinite dilution (eqn (3b)) resulting in eqn (5a):

$$K_{oc} f_{oc} = K_p^{H,hydr} = K_{p,0}^{L,hydr} = K_L^{hydr} C_{s,hydr}^{\max} \quad (5a)$$

Eqn (5a) shows that K_{oc} is linearly related to K_L^{hydr} and f_{oc} to $C_{s,hydr}^{\max}$. Similarly a linear isotherm of any ionic-polar interaction derived from its corresponding Langmuir isotherm at low concentrations can be related to a still unknown sediment parameter, f_{sed} and a normalised ionic-polar sorption parameter, eqn (5b):

$$K_L^{elec} C_{s,elec}^{\max} = K_{p,0}^{L,elec} = K_p^{H,elec} = K_{elec}^{norm} f_{sed} \quad (5b)$$

Eqn (5a) and (5b) gives the possibility to compare Langmuir sorption constants, K_L , from different types of sorption processes. Possible sediment parameters, f_{sed} , that might be related to $C_{s,elec}^{\max}$ will be discussed later.

2.2.3 Virial isotherm. The Virial isotherm⁵ is similar to a linear isotherm with an exponential factor where the exponential form is related to the non-polar correction factor of the ionic-polar interaction, eqn (6):

$$C_s = K_p^V C_w \exp[-b C_s] \quad (6)$$

In this model the parameter b is related to the capacitance of the ionic-polar model. At infinite solution ($C_s, C_w \rightarrow 0$) eqn (6) can be rewritten as eqn (7):

$$C_{s \rightarrow 0} = K_p^V C_{w \rightarrow 0} (1 - b C_{s \rightarrow 0}) \rightarrow C_{s \rightarrow 0} = \frac{K_p^V \frac{1}{b} C_{w \rightarrow 0}}{\frac{1}{b} + K_p^V C_{w \rightarrow 0}} \quad (7)$$

Eqn (7) shows that in a dilute system eqn (6) becomes equivalent to the Langmuir isotherm, eqn (4), and thus that K_p^V is equivalent to $K_{p,0}^{L,Virial}$ and $1/b = C_{s,Virial}^{\max}$. There are two disadvantages in using the Virial over the Langmuir isotherm. Firstly it is difficult to linearize the Virial isotherm and to derive the Virial sorption parameters K_p^V and b . Secondly it will be described below that the way the correction factor for the non-polar interaction is introduced, corresponds only to the DM model.

2.2.4 Freundlich isotherm. When a plot of $\log C_s$ vs. $\log C_w$ is found to be linear a Freundlich isotherm is observed. The Freundlich equation is then given by $C_s = K_F C_w^n$. The Freundlich isotherm is an empirical relationship between the C_w and the C_s , the mechanism underlying the sorption process is not explained. Reported Freundlich isotherms (with surfactants) at environmentally relevant concentrations indicate in nearly all cases a value of $n < 1$.²⁹ When $n < 1$ and $C_w \rightarrow 0$ (physically equivalent to infinite dilution) C_s does not exist. Therefore when $n < 1$ one cannot derive the Freundlich sediment-water partition coefficient at infinite dilution, $K_{p,0}^F$ required in developing sorption models. It also remains unclear how the reported Freundlich sorption constants, K_F , and n , can be transformed into the Freundlich sediment-water partition coefficient, K_p^F , required in the ERA model.

2.3 Defining an average and exact partition coefficient K_p

In a sorption experiment a number of data points of the ratio of measured concentration C_s and C_w , C_s/C_w , at equilibrium are



Table 1 The mathematical expressions of different sorption isotherms and their corresponding exact ($K_p = dC_s/dC_w$) and average ($\bar{K}_p = C_s/C_w$) sediment–water partition constants

Type of sorption isotherm	Linear	Non-linear		
	Henry's law	Langmuir	Freundlich	Virial
$C_s = f(C_w)$	$C_s = K_p^H C_w$	$C_s = \frac{K_{p,0}^L C_s^{\max} C_w}{C_s^{\max} + K_{p,0}^L C_w}$	$C_s = K_F C_w^n$	$C_s = K_{p,0}^{L, \text{Virial}} C_w \exp[-bC_s]$
Infinite dilution ($C_s, C_w \rightarrow 0$)	$C_{s \rightarrow 0} = K_p^H C_{w \rightarrow 0}$	$C_{s \rightarrow 0} = K_{p,0}^L C_{w \rightarrow 0}$	Limit does not exist when $n < 1$	$C_{s \rightarrow 0} = \frac{K_{p,0}^{L, \text{Virial}} \frac{1}{b} C_{w \rightarrow 0}}{\frac{1}{b} + K_{p,0}^{L, \text{Virial}} C_{w \rightarrow 0}}$
Exact K_p at each C_w ($K_p(C_w)$)	$K_p^H = \frac{C_s}{C_w}$	$K_p^L = \frac{K_{p,0}^L (C_s^{\max})^2}{(C_s^{\max} + K_{p,0}^L C_w)^2}$	$K_p^F = n K_F C_w^{n-1}$	$K_p^V = \frac{K_{p,0}^{L, \text{Virial}} \exp[-bC_s]}{b K_{p,0}^{L, \text{Virial}} C_w \exp[-bC_s] + 1}$
Average K_p at each C_w ($\bar{K}_p(C_w)$)	$\bar{K}_p^H = \frac{C_s}{C_w}$	$\bar{K}_p^L = \frac{K_{p,0}^L C_s^{\max}}{C_s^{\max} + K_{p,0}^L C_w}$	$\bar{K}_p^F = K_F C_w^{n-1}$	$\bar{K}_p^V = K_{p,0}^{L, \text{Virial}} \exp[-bC_s]$

established (eqn (1)). However mathematically one determines the K_p value for each data point as the ratio of the difference in C_s and C_w between two data points being the measured value and the origin, $K_p = \Delta C_s / \Delta C_w$. In case K_p is determined by establishing a ratio between the measured value and the origin or between two distinct sorption data, we refer in this article to an average K_p : \bar{K}_p .

When a mathematical equation is established between the measured data points it is possible to obtain both the C_s and K_p at each C_w , $C_s(C_w)$ and $K_p(C_w)$. Establishing the mathematical relationship between the measured data points is mathematically equivalent to taking the limiting value of ΔC_w to zero, $\Delta C_w \rightarrow 0$. In this case the $K_p(C_w)$ can be established by taking the differential of $C_s(C_w)$, dC_s/dC_w . In this study we speak then of an exact K_p . Although such an approach has been reported once for surfactants in the scientific literature⁵ it has not been elaborated further upon. In the literature invariably average K_p values (\bar{K}_p) (e.g. ref. 30 and 31) are being reported, but it is the exact K_p that needs to be used in the development of sorption models and in ERA models. An exact $K_p(C_w)$ at each C_w is therefore obtained by differentiating C_s to C_w , dC_s/dC_w , while the average K_p ($\bar{K}_p(C_w)$) at each C_w is obtained by dividing C_s over C_w , $C_s(C_w)/C_w$. Exact and average partition coefficients of the most commonly used sorption isotherms are shown in Table 1. From here on K_p refers to an exact partition coefficient unless specifically indicated otherwise.

2.4 $\Delta_s G_{\text{total}}^0$ and K_p^{total} of the IM and DM model

The two interaction modes, depicted in Fig. 1, allow to establish the overall standard free enthalpy of the sorption process and the corresponding partition coefficients, the overall sorption isotherms and their behaviour at infinite dilution to derive the different partition coefficients, K_p^{elec} , and K_p^{hydr} with the adsorbent (see Table 2).

The equations in Table 2 are the final equations used in this study to construct and explain observed differences in the adsorption and desorption behaviour of surfactants with

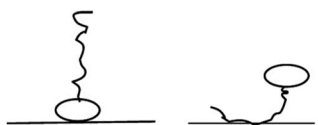

sediments at low concentrations. For the overall isotherm in the IM model a Langmuir isotherm for the ionic-polar interaction and a Henry's law isotherm for the non-polar interaction have been selected instead of two Langmuir isotherms. In Section 4.1 it will be justified when such an approach is feasible. However the procedure is equivalent if the non-polar interaction is given by a non-polar Langmuir isotherm. The IM model describes the sorption process in the experimental system by two completely different types of sorption sites on the same sediment or two different types of sediment, each with a specific $K_{p,0}$ and C_s^{\max} . In contrast, the DM model describes the experimental system by one adsorbent (e.g. organic matter) and one type of sorption location with one specific $K_{p,0}$ and C_s^{\max} where both type of interactions take place simultaneously. Because these experimental systems are different, the thermodynamic overall equations and the overall equations of the partition coefficients of each system are different. Table 2 shows that $\Delta_s G_{\text{total}}^0$ for the DM model is a simple addition of the non-polar and ionic-polar process while this is not the case for the IM model. Otherwise stated, the total sorption coefficient K_p^{total} is the sum of the non-polar and ionic-polar partition coefficient for the IM model, while it is the product of the non-polar and ionic-polar partition coefficient for the DM model.

2.5 From experimental system parameter, $K_{p,0}$, to its molecular sorption parameter(s), K

If the $K_{p,0}$ -value must be related to its corresponding molecular sorption constant the value must also be corrected for its system parameter(s) because a change of thermodynamic system is considered. Therefore the K_L in the Langmuir equation (cf. eqn (3)) is equivalent to the molecular sorption constant and these equilibrium values must be used as input for molecular sorption models and SARs. This procedure is equivalent to what is a common procedure in environmental chemistry: to normalise measured partition coefficients directly on the (dissolved) organic carbon (cf. eqn (5a)). However such a procedure of normalisation on organic carbon is allowed if it is *assured* that



Table 2 Overview of the two proposed modes of interaction of surfactant molecules with sediments, the corresponding overall sorption constants, K_p^{total} and the standard free enthalpy changes for the applied experimental system, $\Delta_s G_{\text{total}}^0$. See Section 4.1 under what experimental conditions a Henry's law (linear) isotherm can be applied for the non-polar interaction in the independent mode model

	Independent mode	Dual-mode
Molecular sorption model		
Overall standard free enthalpy change, $\Delta_s G_{\text{total}}^0$, of the sorption process	$\Delta_s G_{\text{total}}^0 = -RT \ln \{ \exp(-\Delta_s G_{\text{elec}}^0/RT) + \exp(-\Delta_s G_{\text{hydr}}^0/RT) \}$	$\Delta_s G_{\text{total}}^0 = \Delta_s G_{\text{elec}}^0 + \Delta_s G_{\text{hydr}}^0$
Overall partition coefficient, K_p^{total}	$\frac{C_s^{\text{tot}}}{C_w} = \frac{C_s^{\text{elec}}}{C_w} + \frac{C_s^{\text{hydr}}}{C_w} = K_p^{\text{elec}} + K_p^{\text{hydr}} = K_p^{\text{total}}$ (In general $K_p^{\text{total}} = \sum_i K_p^i$)	$K_p^{\text{total}} = K_p^{\text{elec}} K_p^{\text{hydr}}$ or $\ln K_p^{\text{total}} = \ln K_p^{\text{elec}} + \ln K_p^{\text{hydr}}$ (In general: $K_p^{\text{total}} = \prod_i K_p^i$)
Overall sorption isotherm assuming a linear $K_p^{\text{H,hydr}}$	$C_s^{\text{tot}} = \frac{K_{p,0}^{\text{elec}} C_{s,\text{elec}}^{\text{max}} C_w}{C_{s,\text{elec}}^{\text{max}} + K_{p,0}^{\text{elec}} C_w} + K_p^{\text{H,hydr}} C_w$	$C_s = \frac{K_{p,0}^{\text{total}} C_s^{\text{max}} C_w}{C_s^{\text{max}} + K_{p,0}^{\text{total}} C_w}$
Sorption behaviour at infinite dilution ($C_w \rightarrow 0$) assuming a linear $K_p^{\text{H,hydr}}$	$C_s^{\text{total}} = K_{p,0}^{\text{elec}} C_w + K_p^{\text{hydr}} C_w = (K_{p,0}^{\text{elec}} + K_p^{\text{hydr}}) C_w = K_{p,0}^{\text{total}} C_w$	$C_s = K_{p,0}^{\text{total}} C_w = (K_{p,0}^{\text{elec}} K_p^{\text{hydr}}) C_w$
Overall exact partition coefficient, K_p^{total} , assuming a linear $K_p^{\text{H,hydr}}$	$K_p^{\text{tot}} = \frac{K_{p,0}^{\text{elec}} (C_{s,\text{elec}}^{\text{max}})^2}{(C_{s,\text{elec}}^{\text{max}} + K_{p,0}^{\text{elec}} C_w)^2} + K_p^{\text{H,hydr}}$	$K_p^{\text{tot}} = \frac{K_{p,0}^{\text{total}} (C_s^{\text{max}})^2}{(C_s^{\text{max}} + K_{p,0}^{\text{total}} C_w)^2}$

a non-polar interaction takes place. It seems that this procedure is not always applied correctly in sorption studies with surfactants where ionic-polar interactions are also expected.^{22,32–34} Incorrect conclusions on molecular sorption strength will also be drawn if variations in $K_{p,0}$ -values are not corrected for the system parameter C_s^{max} when different adsorbents are used.^{35,36}

The standard free enthalpy of the molecular sorption processes, $\Delta_s G_L^0$, can be calculated from the corresponding K_L -value, $\Delta_s G_L^0 = -RT \ln K_L$. This standard free enthalpy can only be calculated correctly if K_L is dimensionless. Usually K_L -values are reported in L mol^{-1} . However, there is no general method to modify to a unit-less value. It is then difficult to compare similar $\Delta_s G_L^0$ -values from different references³⁷ and erroneous conclusions may be drawn on the nature of the sorption process. There has been consensus on the direct use of the unit L mol^{-1} for non-ionic and dilute ionic solutions because the activity coefficient does not vary too much.³⁸ In colloid chemistry K_L -values are often transformed into a “dimensionless” value of mol mol^{-1} by transforming the liter-unit of water into mol-unit ($1 \text{ L water} = 55.5 \text{ mol water}$ if the experiment was conducted in an aqueous solution). However Azizian recently challenged this transformation because a mol of an adsorbate is not equivalent to a mol of water.³⁹ In his kinetic derivation of the Langmuir-equation he proposed to introduce a relative $C_r(t)$ instead of a $C_w(t)$ based on the maximum solubility of the solute in water, $C_{\text{aq}}^{\text{sat}}$, $C_r(t) = C_w(t)/C_{\text{aq}}^{\text{sat}}$. The modified (thermodynamic)

Langmuir isotherm with a real dimensionless Langmuir constant, K_{ML} , will appear then as (eqn (8)):

$$C_s = \frac{C_s^{\text{max}} K_{\text{ML}} C_w}{(C_{\text{aq}}^{\text{sat}} - C_w) + K_{\text{ML}} C_w} \quad (8)$$

Although appealing, it is not clear how the term $C_{\text{aq}}^{\text{sat}}$ must be interpreted in the case of possible micellization.

The influence of a non-polar and ionic-polar interaction on $\Delta_s G^0$ when the number of CF_2 or CH_2 units in the tail of the surfactant is varied, can be described as follows. If $K_{p,0}$ -values of *only* an ionic-polar interaction of the surfactant with the adsorbent, $K_{p,0}^{\text{elec}}$, are established then the standard free enthalpy variation of e.g. an addition of CF_2 -unit (N_{CF_2}) in the tail, $\Delta \Delta_s G_{L,\text{tail}}^0$, is given by a contribution of the head which is adsorbed to the sorbent and the tail in the water cf. eqn (9a)

$$\Delta_s G_{p,\text{elec}}^0(N_{\text{CF}_2}) = \Delta_s G_{L,\text{head-sorbent}}^0 + \Delta \Delta_s G_{L,\text{head-sorbent}}^0 N_{\text{CF}_2} - RT \ln C_{s,\text{elec}}^{\text{max}} \quad (9a)$$

and similarly for *only* a non-polar interaction with the adsorbent, $K_{p,0}^{\text{hydr}}$, by eqn (9b).

$$\Delta_s G_{p,\text{hydr}}^0(N_{\text{CF}_2}) = \Delta_s G_{L,\text{tail-sorbent}}^0 + \Delta \Delta_s G_{L,\text{tail-sorbent}}^0 N_{\text{CF}_2} - RT \ln C_{s,\text{hydr}}^{\text{max}} \quad (9b)$$



In case of K_L -values, the term $-RT \ln C_s^{\max}$ would not appear in eqn (9a) and (9b). When in the applied experimental system *both* interactions occur at the same time, the observed value of $\Delta\Delta_s G_{L, \text{observed}}^{0, \text{CF}_2}$ for the IM model will differ from the DM model.

The fact that in a sorption experiment two thermodynamic systems must be considered has also a profound influence on its adsorption or desorption rate processes. In any rate measurement it is the experimental system which relaxes to equilibrium. In the study of Azizian⁴⁰ where the Langmuir rates of adsorption (k_a) and desorption (k_d) are directly linked to $C_s(t)$, it can be shown that when $C_w(0) \gg C_s(0)$ *i.e.*, when the initial concentration of the solute in the water phase is very high compared to the adsorbed one, the experimentally observed rate constant is of pseudo-first order and is a combination of the adsorption and desorption Langmuir rate constants. Both Langmuir rate constants can be obtained by plotting the observed rate constant *vs.* the initial concentration of the solute, $C_w(t=0)$, which should lead to a straight line with k_a as slope and k_d as intercept and therefore establish the Langmuir sorption constant, K_L , in another way. Owing to the existence of different kinetic regimes it is not necessary that the kinetically derived K_L and the thermodynamically derived K_L lead to similar values. In the same ref. 40 it is also shown that when $C_w(0) \geq C_s(0)$ or when the initial concentration of the solute is not too high a pseudo-second-order model is observed which leads to the Langmuir adsorption isotherm expression at equilibrium. The observed second-order rate constant is a more complex function of the initial concentration of the solute than in the case of the first-order rate constant. There are several ways to show that the Langmuir adsorption and desorption rate process are of a second order nature. In this study the derivation is given in Annex II.

3. Model application to several sorption phenomena

3.1 Overview

As stated before, well-defined substance and/or sediment parameters can be derived from the Langmuir, Henry's law and

Virial isotherms at infinite dilution. Therefore only sorption data derived from these three isotherms are relevant in the model development. In addition, sorption isotherms should be established at low, and preferably at environmentally relevant, surfactant concentrations. In order to avoid experimental artefacts, direct analysis of both the sediment and water phase should have been applied. The resulting data set is small despite the large number of references dealing with sorption of surfactants to sediment (*cf.* Table S1, ESI†). In Table S1† the $K_{p,0}^{\text{total}}$ of Matthijs *et al.*⁴¹ are calculated from their reported K_L and C_s^{\max} values for the anionic surfactant C12-LAS (*cf.* eqn (3b)).

– Section 3.2 describes then how the sorption of surfactants is influenced by various organic carbon fractions according to the IM and DM model, using the anionic surfactant C12-LAS as an example. Reported sorption values for LAS from the literature at very low and very high contents of organic carbon^{26,41–43} will be used to derive their model-specific partition coefficients, $K_{p,0}^{\text{hydr}}$, $K_{p,0}^{\text{elec-IM}}$ and $K_{p,0}^{\text{elec-DM}}$. After deriving the model partition coefficients, the IM and DM isotherms will be constructed again according to Table 2 by varying the organic carbon fraction (1%, 10%, 20%). The curvature at infinite dilution and the overall isotherms over the full concentration range will then be compared to experimentally observed isotherms.

– In Section 3.3, the influence of surfactants head groups and/or tail length is discussed. In Section 3.3.1 the overall sorption isotherms according to the IM and DM model of a mixture of nonylphenol ethoxylates (NPEO_x) as an example where only the head varies will be constructed and compared to similar reported isotherms. In Section 3.3.2 sorption data of a mixture of LAS as an example of varying tail lengths will be compared to the individual components of the mixture.

– In Section 3.4, the incremental standard free enthalpy values ($\Delta\Delta_s G_{L, \text{tail}}^{0, \text{CF}_2}$) reported on varying the number of CF₂-groups of perfluorinated carboxylated acids (PFCAs), will be compared to experimentally observed values when both interactions are present.

– In Section 3.5, the influence of different adsorbents on the experimentally observed adsorption isotherm will be given, and particularly will discuss how different sorption processes influence the desorption rate isotherms.

Table 3 C12-LAS IM and DM model parameters with $f_{oc} = 1\%$, 10% and 20% and $K_{oc} = 1500 \text{ L kg}^{-1}$. $K_{p,0}^{\text{total}} = 211 \text{ L kg}^{-1}$ for case 0 obtained by multiplying a and b from Table 6 for sediment 2 in Matthijs.⁴¹ In italics $K_{p,0}^{\text{hydr}}$ calculated from $K_{oc}f_{oc}$. In bold $K_{p,0}^{\text{elec}}$ values calculated according to the IM ($K_{p,0}^{\text{hydr}} + K_{p,0}^{\text{elec}} = K_{p,0}^{\text{total}}$) or DM ($K_{p,0}^{\text{hydr}}K_{p,0}^{\text{elec}} = K_{p,0}^{\text{total}}$) model from $K_{p,0}^{\text{hydr}}$ and the experimentally derived $K_{p,0}^{\text{total}}$ (case 0). $K_{p,0}^{\text{total}}$ in case 1 to 6 are calculated from $K_{p,0}^{\text{hydr}}$ and $K_{p,0}^{\text{elec}}$ values according to the IM model and DM model for the different organic carbon fractions

Case	f_{oc}	$K_{p,0}^{\text{hydr}}$ (L kg ⁻¹)	$K_{p,0}^{\text{elec-IM}}$ (L kg ⁻¹)	$K_{p,0}^{\text{elec-DM}}$ (L kg ⁻¹)	$K_{p,0}^{\text{total}}$ (L kg ⁻¹)	Remark
0	1%				211	From cited values (Matthijs ⁴¹)
1	1%	15	14		211	$K_{p,0}^{\text{hydr}}$ see text. $K_{p,0}^{\text{elec}}$ based on DM-model
2	1%	15	196		211	$K_{p,0}^{\text{hydr}}$ see text. $K_{p,0}^{\text{elec}}$ based on IM-model
3	10%	150	196		346	$K_{p,0}^{\text{elec-IM}}$ constant and using IM model to estimate $K_{p,0}^{\text{total}}$
4	20%	300	196		496	$K_{p,0}^{\text{elec-IM}}$ constant and using IM model to estimate $K_{p,0}^{\text{total}}$
5	10%	150		14	2100	$K_{p,0}^{\text{elec-DM}}$ constant and using DM model to estimate $K_{p,0}^{\text{total}}$
6	20%	300		14	4200	$K_{p,0}^{\text{elec-DM}}$ constant and using DM model to estimate $K_{p,0}^{\text{total}}$



– In Section 3.6, a few published examples will be discussed where both a non-polar and ionic-polar Langmuir isotherm were observed.

3.2 Applying the IM and DM model to variable OC contents

3.2.1 Deriving K_p^{IM} and K_p^{DM} partition coefficients for anionic surfactant C12-LAS. For the non-polar interaction, the linear isotherms with the anionic surfactant LAS and an organic carbon rich sorption material (22% and 40% respectively), a non-polar partition coefficient for C12-LAS of around $K_{\text{oc}} = 1500 \text{ L kg}^{-1}$ can be derived with eqn (5).^{43,44} At very low organic carbon fractions, the isotherm is often strongly non-linear and can be described by a single Langmuir isotherm. This has also been observed for LAS.⁴¹ The Langmuir values of the sediment 2 in that study, that contained a f_{oc} of 0.01 are applied here. On using these reported Langmuir values in eqn (3b), K_L ($0.11 \text{ mL } \mu\text{g}^{-1}$) and $C_{\text{s,elec}}^{\text{max}}$ ($1923 \text{ } \mu\text{g g}^{-1}$), the overall partition coefficient for C12-LAS, at infinite dilution can be calculated $K_{\text{p},0}^{\text{total}} = 0.11 \times 1923 = 211 \text{ L kg}^{-1}$. In the overall isotherm of both the IM and DM model the ionic-polar interaction of the head is present (Table 2). Therefore the value of $C_{\text{s}}^{\text{max}}$ should be the same in both model equations at this specific experiment leading to the same $K_{\text{p},0}^{\text{total}}$ at infinite dilution for both models. On using a $K_{\text{oc}} = 1500 \text{ L kg}^{-1}$ and a $f_{\text{oc}} = 0.01$, $K_p^{\text{hydr}} = 15 \text{ L kg}^{-1}$ is derived in this particular experiment. With this value and the observed $K_{\text{p},0}^{\text{total}} = 211 \text{ L kg}^{-1}$, the value of $K_{\text{p},0}^{\text{elec}}$ according to the IM ($K_{\text{p},0}^{\text{elec-IM}}$) or DM ($K_{\text{p},0}^{\text{elec-DM}}$) model can be derived using the overall partition coefficients at infinite dilutions from Table 2: $K_{\text{p},0}^{\text{elec-IM}} = 211 - 15 = 196 \text{ L kg}^{-1}$ and $K_{\text{p},0}^{\text{elec-DM}} = 211/15 = 14 \text{ L kg}^{-1}$ respectively. Comparing the calculated values of $K_{\text{p},0}^{\text{elec-IM}}$ and $K_{\text{p},0}^{\text{elec-DM}}$ with K_p^{hydr} shows that the ionic-polar sorption strength of LAS is dominant in the IM model while in the DM model both the ionic-polar and non-polar sorption values are of the same order of magnitude. On using the derived values of $K_{\text{p},0}^{\text{elec-DM}}$ and $K_{\text{p},0}^{\text{elec-IM}}$ one can also calculate $K_p^{\text{total-IM}}$ and $K_p^{\text{total-DM}}$ on increasing the f_{oc} from 1% to 10% and 20%. Table 3 shows these derived partition

coefficients. These values will be used to construct different overall sorption isotherms.

3.2.2 IM and DM sorption isotherms on increasing the organic carbon content. The overall IM and DM sorption isotherms of LAS derived from the IM and DM partition coefficient from Table 3 for the organic carbon fractions of 1%, 10% and 20% are depicted in Fig. 2 in the experimentally applied concentration range from $1\text{--}10 \text{ mg L}^{-1}$.

Fig. 2b shows that upon increasing the organic carbon fraction the DM model remains a Langmuir isotherm albeit the isotherms become steeper at the origin. Therefore the curvature of the DM isotherms at low concentrations increases on increasing the organic carbon fraction. This is in contradiction to the isotherms constructed by the IM model (Fig. 2a). This one indicates that the isotherms become more linear near the origin on increasing f_{oc} . Such a difference in isotherm behaviour can also be extended to the Freundlich isotherm. If the DM model is valid an increase in organic carbon would lead to a change in n further from 1 but if the IM model is valid, n would become closer to 1 and the isotherm becomes more linear. This increase in linearity and n to values closer to 1 on increasing the oc-fraction is observed clearly *e.g.* for C12-LAS⁵ and for the per-fluorinated sulphonates⁴⁵ but much less for A_{13}EO_6 .⁴⁶ The IM model explains the observed sorption behaviour as a function of the organic carbon fraction when both types of interaction are present, while the DM model does not.

When deriving the IM and DM partition coefficients for f_{oc} of 0.01 from the experimental data of Matthijs (1985),⁴¹ the observed overall isotherm according to the DM model with $K_{\text{p},0}^{\text{total}} = 211 \text{ L kg}^{-1}$ and $C_{\text{s,elec}}^{\text{max}}$ of 1923 mg kg^{-1} , is nearly equivalent to the IM model isotherm (from eqn (4)) with $K_{\text{p},0}^{\text{elec-DM}} = 196 \text{ L kg}^{-1}$ and $C_{\text{s,elec}}^{\text{max}}$ of 1923 mg kg^{-1} , including a linear part with $K_p^{\text{hydr}} = 15 \text{ L kg}^{-1}$. The IM model leads to a difference between the experimental C_s and the calculated one of around 14% only at the highest applied concentration (15 mg L^{-1}). Both isotherms are shown in Fig. 2a (case 0 and 2 respectively). It can be concluded here that the difference in C_s calculated by the IM

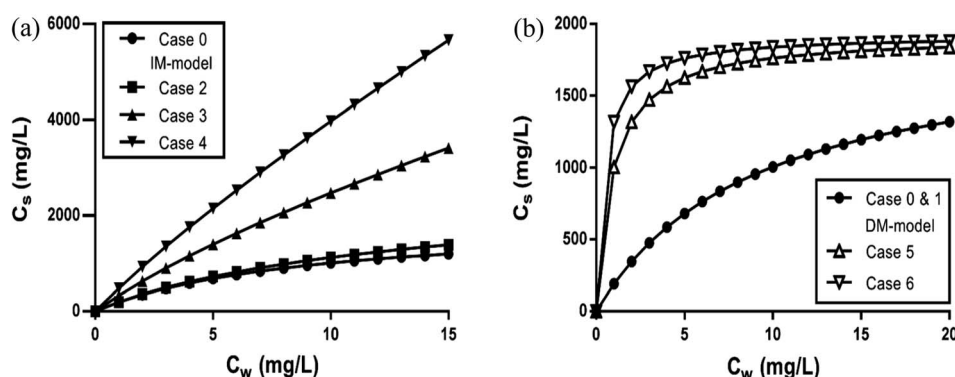


Fig. 2 C12-LAS overall sorption isotherms on varying the organic carbon fraction (1% for case 0–2; 10% for case 3 and 5; 20% for case 4 and 6) in the IM model (a) or DM model (b) in the range from 0–15 mg L^{-1} . Case 0 is based on the sediment partition coefficient values observed in Matthijs⁴¹ with $K_{\text{p},0}^{\text{total}} = 211 \text{ L kg}^{-1}$ and $f_{\text{oc}} = 1\%$, from which the $K_{\text{p},0}^{\text{elec}}$ are derived for both the IM and DM model. Case 1 and 2 represent the two model sorption isotherms with 1% organic carbon as used in that study, whereas new sediment compositions with 10 and 20% are simulated based on these obtained $K_{\text{p},0}^{\text{elec}}$ values for both models. The K_p^{hydr} values increase proportional to f_{oc} and are equal for the IM and DM model, $K_{\text{p},0}^{\text{elec}}$ values are constantly 196 L kg^{-1} for IM, and constantly 14 L kg^{-1} for DM (details given in Table 3).



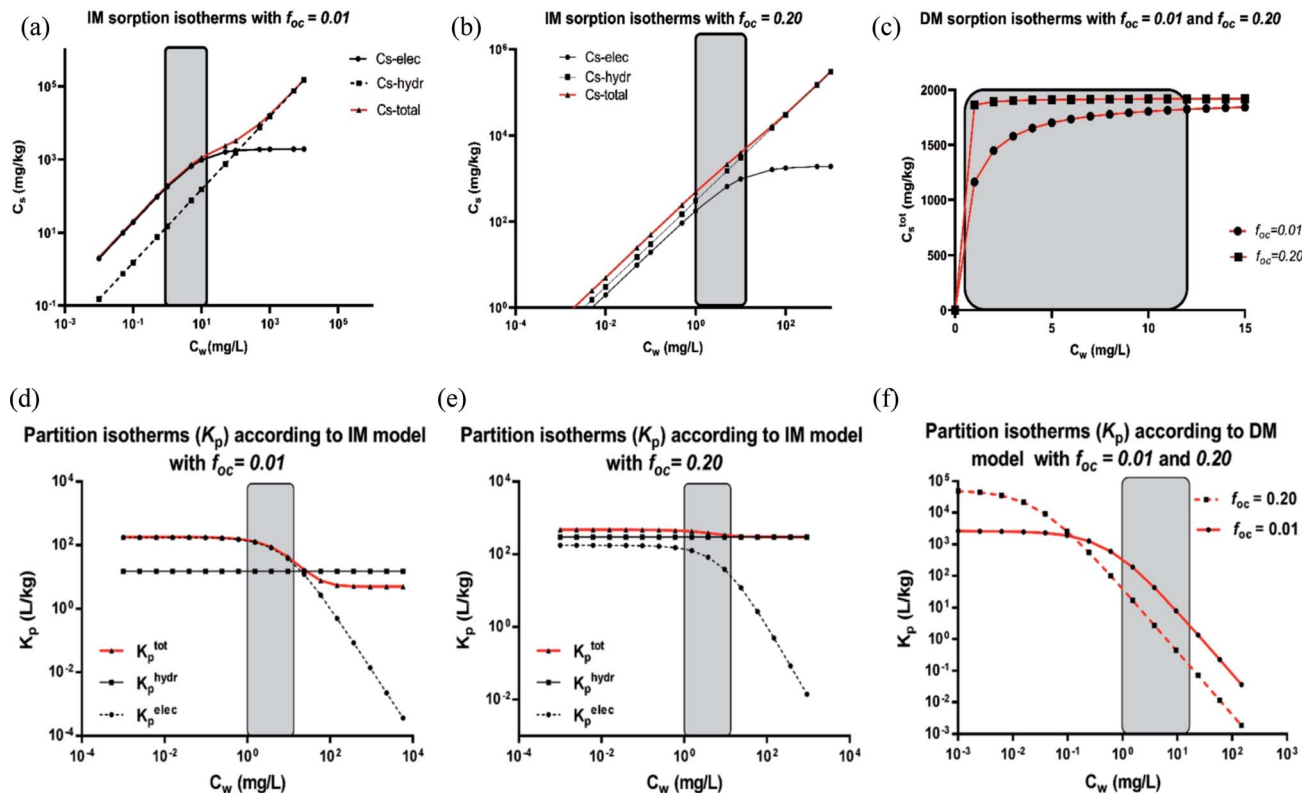


Fig. 3 (a–c) Sorption isotherms of LAS according to the IM and DM model with $f_{oc} = 1\%$ and $f_{oc} = 20\%$ respectively. (a and b) For the IM model, $K_{p,0}^{elec} = 196 \text{ L kg}^{-1}$, $C_s^{max} = 1923 \text{ mg kg}^{-1}$, $K_{oc} = 1500$ with $f_{oc} = 1\%$ (a) and $f_{oc} = 20\%$ (b). (a) and (b) include the separated adsorption isotherms of the electrostatic and hydrophobic interaction and the overall sorption isotherm. (c) shows the sorption isotherms for the DM model with $f_{oc} = 1\%$ and $f_{oc} = 20\%$. The applied experimental concentration range by Matthijs⁴¹ for $f_{oc} = 1\%$ and for $f_{oc} = 20\%$ by Marchesi⁴⁴ are indicated by the grey area. (d–f) Partition isotherms of LAS according to the IM and DM model with $f_{oc} = 1\%$ to $f_{oc} = 20\%$ respectively. (d and e) For the IM model, $K_{p,0}^{elec} = 196 \text{ L kg}^{-1}$, $C_s^{max} = 1923 \text{ mg kg}^{-1}$, $K_{oc} = 1500$ with $f_{oc} = 1\%$ (d) and $f_{oc} = 20\%$ (e). (d) and (e) include the separated partition isotherms of the electrostatic and linear hydrophobic interaction and the overall sorption isotherm. (f) shows the partition isotherms for the DM model with $f_{oc} = 1\%$ and $f_{oc} = 20\%$ respectively. The applied experimental concentration range by Matthijs⁴¹ for $f_{oc} = 1\%$ and for $f_{oc} = 20\%$ by Marchesi⁴⁴ are indicated by the grey area.

or the DM model applied to these experimental data will become only pronounced at higher oc-fractions.

3.2.3 Overall IM or DM sorption and partition isotherms at full concentration range. Fig. 3 shows the overall and separate ionic-polar and non-polar sorption and partition isotherms according to both models over a much larger concentration range than applied above in Section 3.2.2 for two different organic carbon fractions (1% and 20%).

Fig. 3 shows that on using the IM model and depending on the applied concentration range and the characteristics of the sediment, the sorption process can be dominated by the ionic-polar or the non-polar interaction. For example, in Fig. 3a and d it is shown that in the experimental concentration range applied by Matthijs *et al.* (1985)⁴¹ (1–15 mg L⁻¹) the total adsorbed LAS fraction and the overall partition coefficient are dominated by the ionic-polar contribution, whereas at much higher surfactant concentrations (>500 mg L⁻¹) the total adsorbed fraction and the overall partition coefficient is dominated by the non-polar contribution. If the authors would have considered a much larger concentration range (their experimental data would allow such a consideration) then the typical

characteristic S-curvature for the overall sorption isotherm would have been obtained that was observed by other authors *e.g.* ref. 46. At much higher oc-fractions, as in the experiments conducted by *e.g.* Marchesi,⁴⁴ in the IM-model the total adsorbed LAS fraction and the overall partition coefficient is entirely determined by the non-polar interactions over the full concentration range, even at a very low concentration (see Fig. 3b and e). The contribution of the ionic-polar interaction does not play any significant role. This is in contradiction to the DM isotherms constructed from the same data. In both cases ($f_{oc} = 1\%$ and 20%) the sorption and the partition isotherms remain a Langmuir curve over the full concentration range (see Fig. 3c and f).

We conclude here that the IM model can explain several features in observed sorption isotherms of surfactants at different applied concentration ranges.

3.3 Applying the IM and DM model to variable surfactant structures

3.3.1 Mixture of varying heads but equivalent tail. In this section an interpretation is presented of the data from John⁴⁷



Table 4 $K_{p,0}^{H,elec}$ and $K_{p,0}^{H,hydr}$ for NPEO_{3–12} derived according to the IM model ($K_{p,0}^{H,elec} + K_{p,0}^{H,hydr} = K_{p,0}^{total}$). In italics estimated $K_{p,0}^{H,hydr}$ -values for NPEO_{10–12} from the log K_{oc} vs. N_{EO} correlation from Fig. S1a. The calculated $K_{p,0}^{H,hydr}$ values from the reported data for NPEO_{10–12} are unrealistic because the error in the reported data is in the same range as the expected $K_{p,0}^{H,hydr}$. Using the improved $K_{p,0}^{H,hydr}$ -values for NPEO_{10–12} lead to a set of improved data. Data taken from John⁴⁷

NPEO _x	Reported data (+SE)			Improved data					
	$K_{p,0}^{H,elec}$ (L kg ^{−1})	$K_{p,0}^{total}$ (IM) (L kg ^{−1})	$K_{p,0}^{H,hydr}$ (L kg ^{−1})	$K_{p,0}^{H,hydra}$ (L kg ^{−1})	$K_{p,0}^{total}$ (IM)	$K_{p,0}^{H,hydr}$ (L kg ^{−1})	K_{oc}	log K_{oc}	log $K_{p,0}^{H,elec}$
3	230 + 20	1460 + 140	1230		1460	1230	6150	3.79	2.36
4	270 + 20	930 + 60	660		930	660	3300	3.52	2.43
5	320 + 30	750 + 110	430		750	430	2150	3.33	2.51
6	360 + 40	700 + 70	340		700	340	1700	3.23	2.56
7	330 + 60	590 + 60	260		590	260	1300	3.11	2.52
8	400 + 60	550 + 60	150		550	150	750	2.88	2.60
9	460 + 60	540 + 60	80		540	105	526	2.72	2.66
10	480 + 60	450 + 80	−30?	71	551	71	357	2.55	2.68
11	530 + 90	550 + 110	20?	49	579	49	243	2.38	2.72
12	590 + 120	750 + 180	160?	33	623	33	165	2.22	2.77

^a From NPEO_{10–12} from log K_{oc} vs. N_{EO} QSAR (see ESI Fig. S1). ? = doubtful values because the actual value is within the SE limits.

where Henry's law sediment–water partition coefficients were established for NPEO_{3–12} using a specific size fraction of river sediment in the presence and absence of the organic carbon fraction with $f_{oc} = 0.20$. Partition coefficients measured in the organic free fraction are considered to be caused by an ionic-polar adsorption process of the EO-chain, $K_p^{H,elec}$. Partition coefficients of the native sediment are considered to be caused by a combined ionic-polar and non-polar sorption process, $K_p^{H,total}$. According to the IM model both $K_p^{H,elec}$ and $K_p^{H,hydr}$ can be calculated easily from the reported data for NPEO_{3–9} (see Table 4). Above NPEO₉ however the $K_p^{H,hydr}$ values calculated by the IM model show an erratic behaviour (indicated by question marks in Table 4) even including a negative value that is theoretically impossible. This is caused by the fact that absolute value of the latter K_p values are in the same order of magnitude of the stated error. Therefore the $K_p^{H,hydr}$ -values for NPEO with more than 9 EO units are estimated from the observed high linear correlation between log K_{oc} and the number of EO units, N_{EO} , (see Fig. S1†). In bold and in italics the recalculated IM partition coefficients are indicated in Table 4. Table 5 shows the ionic-polar and non-polar partition coefficients when the DM model is used.

Since no value for $C_{s,elec}^{max}$ is cited in the specific reference an arbitrary value of 100 mmol kg⁻¹ is chosen to show the different isotherm behaviour at low and high concentration. The resulting C_s^{total} isotherms for each NPEO_x according to the IM and DM model for a $f_{oc} = 0.20$ are shown in Fig. 4.

Fig. 4 shows that at high C_w (>0.01 mmol L⁻¹) the sequence in the IM model is NPEO₄ > NPEO₈ > NPEO₁₂. In the IM model at high concentration the non-polar interaction is dominant because the ionic-polar sorption process does not contribute anymore to C_s and NPEO₄ shows the largest value of K_{oc} . This is not the case in the DM model where the sequence is NPEO₄ > NPEO₁₂ > NPEO₈ which is also equivalent at low concentrations in the IM model. This is expected as in both models the sequence of the $K_{p,0}^{total}$ values corresponds to NPEO₄ > NPEO₁₂ > NPEO₈. Therefore it can be shown that in the IM model a reversal of the isotherm of NPEO₈ and NPEO₁₂ or on similar grounds for any similar surfactant with the same tail and a varying head can be expected when the full isotherm is established or when the concentration range is high enough that one of the two isotherms (non-polar or ionic-polar) is saturated. Such a reversal phenomenon has indeed been observed for experimental sorption of C₁₂EO_{1,3,5} (ref. 48) and an increasing influence of the organic carbon fraction compared to

Table 5 $K_{p,0}^{H,elec}$ and $K_{p,0}^{H,hydr}$ for NPEO_{3–12} derived according to the DM model ($K_{p,0}^{H,elec} K_{p,0}^{H,hydr} = K_{p,0}^{total}$). Data taken from John⁴⁷

NPEO _x	Reported data (+SE)					
	$K_{p,0}^{H,elec}$ (L kg ⁻¹)	$K_{p,0}^{total}$ (DM)	$K_{p,0}^{H,hydr}$ (L kg ⁻¹)	K_{oc}	log K_{oc}	log $K_{p,0}^{H,elec}$
3	230 + 20	1460 + 140	6.35	31.74	1.50	2.36
4	270 + 20	930 + 60	3.44	17.22	1.24	2.43
5	320 + 30	750 + 110	2.34	11.72	1.07	2.51
6	360 + 40	700 + 70	1.94	9.72	0.99	2.56
7	330 + 60	590 + 60	1.79	8.94	0.95	2.52
8	400 + 60	550 + 60	1.38	6.88	0.84	2.60
9	460 + 60	540 + 60	0.98	4.89	0.69	2.66
10	480 + 60	450 + 80	1.15	5.73	0.76	2.68
11	530 + 90	550 + 110	1.42	7.08	0.85	2.72
12	590 + 120	750 + 180	1.08	5.42	0.73	2.77



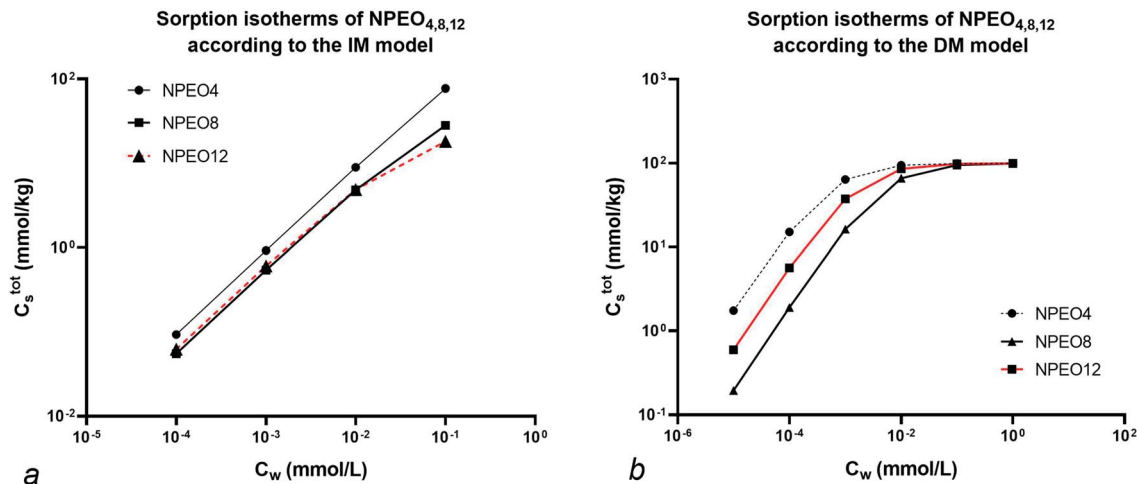


Fig. 4 IM (a) and DM (b) model sorption isotherms of $\text{NPEO}_{x=4,8,12}$. For data see text. Note the reversal in sequence at low concentration with $N_{\text{EO}} = 8$ and $N_{\text{EO}} = 12$ units for the IM model but not for the DM model.

the clay fraction at higher C_w .⁴⁹ In case both the heads and tails vary as in alkylethoxylates (AEO) the chemical variation in AEO at different C_w is much more difficult to model. The IM model can explain reversals of the sequence of isotherms of a mixture of surfactants with different heads and similar tails.

3.3.2 Mixture of equivalent head but varying tail. For a mixture of surfactants with a similar head but varying tail *e.g.* LAS, it is expected that in both models $C_{s,\text{elec}}^{\text{max}}$ will remain equal on a molar base when established at dilute concentrations or with individual surfactants. Within the experimental error this constancy has been demonstrated in all cases of anionic and non-ionic sorption^{5,45,46,50} but not in the case described by Istok *et al.*²⁶ In the latter study the $C_{s,\text{elec}}^{\text{max}}$ values were derived from the Langmuir isotherms of the different LAS components in one experiment over a vast concentration range ($\sim 8000 \text{ mg L}^{-1}$). This range is nearly equivalent to the reported overall $C_{s,\text{elec}}^{\text{max}}$ ($\sim 8600 \text{ mg kg}^{-1}$) of all the individual LAS components. However the reported $C_{s,\text{elec}}^{\text{max}}$ values are not independent from each other since the head of each different LAS is equivalent. This dependence can be explained as follows. At high C_w all sorption sites are occupied and the Langmuir isotherm levels off. In that case the value of K_p^{elec} for each LAS has decreased to $\sim 0 \text{ L kg}^{-1}$ and $C_s = C_{s,\text{elec}}^{\text{max}}$ for each individual LAS. If no sorption interaction

is present anymore for each individual LAS, the number of sorption sites is then only related to the mass ratios of the LAS present in the system. A mixture of 22% C_{10} , 42% C_{11} , 27% C_{12} , and 9% C_{13} LAS alkyl chain homologues was used in the Istok *et al.* experiment. The observed fractions of $C_{s,\text{elec}}^{\text{max}}$ calculated in the present work for each LAS corresponds to $C_{10} = 23\%$, $C_{11} = 40\%$, $C_{12} = 32\%$ and $C_{13} = 5\%$. The results at saturated sorption are equivalent for both models. The model results are equivalent because at high concentrations only one type of sorption process occurs. While this is always the case for the DM model, it is not necessarily the case for the IM model. However, the experimental results show that at these high concentration there is no additional other interaction process (for example, at high concentrations micellar structures may be formed). While the $C_{s,\text{elec}}^{\text{max}}$ of each individual LAS does not change (equivalent head) at infinite dilution the partition coefficient, $K_{p,0}^{\text{elec}}$ still varies because K_L^{elec} varies for each different surfactant.

3.3.3 Derived and observed slope behaviour of a series of PFCA. Several series of partition coefficients of PFCA at infinite dilution and their corresponding $\Delta\Delta_s G_L^{0,\text{CF}_2}$ on pure and complex adsorbents have been reported.^{8,51,52} On a pure ionic-polar adsorbent *e.g.* kaolinite or a weak anion exchanger (WAX) it is assumed that the value of $\Delta\Delta_s G_L^{0,\text{CF}_2}$ can be found by

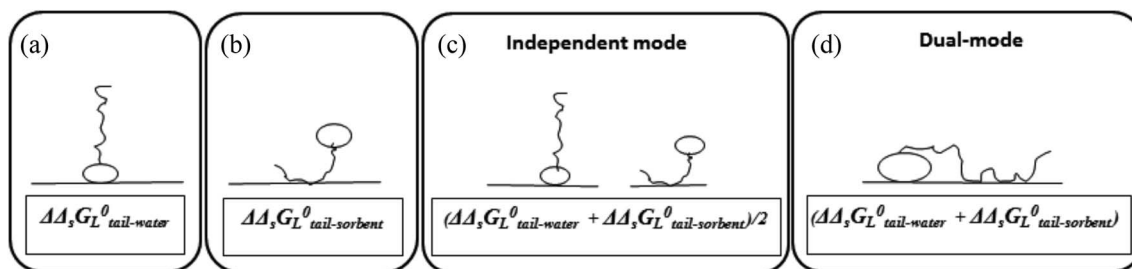


Fig. 5 Schematic representation of how the IM and DM model include the increment in standard free enthalpy for each additional carbon unit in a hydrophobic chain ($\Delta\Delta_s G_L^0$): (a) and (b) individually for the ionic-polar and non-polar interaction, (c) in the IM model, (d) in the DM model (applied to CF_2 in perfluorocarboxylates in this study).



Table 6 Experimental incremental standard free enthalpy, $\Delta_s \Delta G_L^0(\text{CF}_2)$ (kJ mol⁻¹), sorption values of perfluoroalkyl acids on different adsorbent, predicted incremental values for the IM and DM model when both a non-polar and ionic-polar interaction are taking place simultaneously, and observed incremental values

	Only non-polar assumed	Only ionic-polar assumed	Predicted $\Delta_s \Delta G_L^0(\text{CF}_2)$ according to the different models		
	$\Delta_s \Delta G_L^0(\text{CF}_2)^{\text{tail-adsorbent}}$	$\Delta_s \Delta G_L^0(\text{CF}_2)^{\text{head-adsorbent}}$	Dual-mode	Independent mode	Observed $\Delta_s \Delta G_L^0(\text{CF}_2)$
	4.70 ± 0.34 (C18) ^a	2.6 ± 0.24 (WAX) ^a			3.3 (org. matter) ^c
	4.00 ± 0.40 (HLB) ^a	2.5 ± 0.23 (MAX) ^a			3.4 (sediment) ^b
	4.7 (octanol) ^a	2.6 (kaolinite) ^b			
	4.3 (C18) ^d				
Average	4.5	2.6	7.1	3.5	3.4

^a C. Eschauzier.⁵¹ ^b F. Xiao.⁸ ^c C. P. Higgins.¹¹ ^d P. de Voogt.⁵²

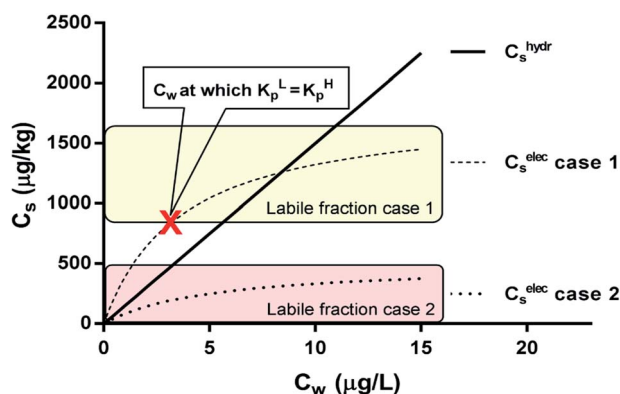


Fig. 6 Two sorption cases of a surfactant according to the IM model. Case 1 is a combination of a linear (non-polar) and Langmuir (ionic-polar) sorption process where the Langmuir isotherm is at least partially above the linear isotherm ($K_{p,0}^{\text{elec}} > K_p^{\text{H,hydr}}$) with $K_p^{\text{H,hydr}} = 150$ L kg⁻¹, $K_{p,0}^{\text{elec}} = 500$ L kg⁻¹ and $C_{s,\text{elec}}^{\text{max}} = 1800$ μg kg⁻¹. Case 2 where the entire Langmuir (ionic-polar) isotherm is below the linear (non-polar) one ($K_{p,0}^{\text{elec}} < K_p^{\text{H,hydr}}$) with $K_p^{\text{H,hydr}} = 150$ L kg⁻¹, $K_{p,0}^{\text{elec}} = 100$ L kg⁻¹ and $C_{s,\text{elec}}^{\text{max}} = 500$ μg kg⁻¹. With these data the C_w for which $K_p^{\text{L,elec}} = K_p^{\text{H,hydr}}$ in case 1 is equal to ~ 3.0 μg L⁻¹ according to eqn (10) and divides the adsorbed ionic-polar fraction into a labile and non-labile one. The labile (ionic-polar) fractions that will be desorbed first because they are weaker bound than the non-polar fraction are indicated by the colored sections.

the slope on applying eqn (9a). On a pure non-polar adsorbent *e.g.* HLB or C18 it is assumed the slope can be found by applying eqn (9b). If both types of interactions take place at the same time then according to the IM model the adsorption processes are independent and the overall incremental value is the average value of both values (Fig. 5c). In case the DM model is considered then both interactions are simultaneously taking place and the overall incremental value is an addition of both values (Fig. 5d).

Table 6 shows reported values of slopes of PFCAs sorption processes on both pure and mixed adsorbents.

Table 6 shows that when both interactions take place the slope follows the IM model and not the DM one.

Established K_L^{elec} or $\Delta_s \Delta G_L^0$ values of cationic or anionic surfactants vary with the ionic strength of the solution. However

this does not count for the slope of a sequence of such type of surfactants $\Delta \Delta_s \Delta G_{L,\text{tail}}^{0,\text{CF}_2}$.⁸

3.4 Applying the IM and DM model to describe desorption processes

As described before in kinetic sorption experiments two thermodynamic systems are present, the experimental one and the molecular one leading to complex molecular rate functions. In this case adsorption and desorption results between the IM and DM model can be quite different because in the IM model two different adsorbents are present each having their independent sorption isotherm.

3.4.1 Labile and non-labile fractions with the IM model. In the case of a combination of a Langmuir isotherm from an assumed ionic-polar sorption process and a Henry's law isotherm from an assumed non-polar sorption process, two cases can be distinguished for the Langmuir isotherm compared to the linear Henry's law isotherm which are depicted in Fig. 6. Case 1 corresponds to a $K_{p,0}^{\text{L,elec}} > K_p^{\text{H,hydr}}$ while the second case corresponds to $K_{p,0}^{\text{L,elec}} < K_p^{\text{H,hydr}}$.

The value of C_w for which both the Langmuir ionic-polar and the Henry's law non-polar isotherm have the same partition coefficient, $K_p^{\text{L,elec}} = K_p^{\text{H,hydr}}$, can be found by equating in this case the exact K_p for the different isotherm (Table 2) leading to eqn (10)

$$C_w^{K_p^{\text{L,elec}} = K_p^{\text{H,hydr}}} = \frac{C_{s,\text{elec}}^{\text{max}}}{K_{p,0}^{\text{L,elec}}} \left(\sqrt{\frac{K_{p,0}^{\text{L,elec}}}{K_p^{\text{H,hydr}}}} - 1 \right) \quad (10)$$

For the data applied in Fig. 6 this is at a C_w of ~ 3 μg L⁻¹. This equation is only valid for $K_{p,0}^{\text{L,elec}} > K_p^{\text{H,elec}}$ corresponding to case 1. The C_w where $K_{p,0}^{\text{L,elec}} = K_p^{\text{H,hydr}}$ divides the non-linear (Langmuir) sorbed fraction in the IM model into two parts, a labile or fast one where $C_w > C_w^{K_p^{\text{L,elec}} = K_p^{\text{H,hydr}}}$ and a non-labile or slow one where $C_w < C_w^{K_p^{\text{L,elec}} = K_p^{\text{H,hydr}}}$. In any desorption experiment above $C_w = C_w^{K_p^{\text{L,elec}} = K_p^{\text{H,hydr}}}$ the first fraction that is removed is the labile ionic-polar adsorbed fraction followed by desorption of the non-polar adsorbed one. However below $C_w = C_w^{K_p^{\text{L,elec}} = K_p^{\text{H,hydr}}}$ the first



Table 7 C_s^{total} , C_s^{hydr} and C_s^{elec} at selected C_w values according to the IM mode assuming a linear non-polar isotherm and Langmuir ionic-polar isotherm for two different cases. Case 1 is when $K_p^{\text{L,elec}} > K_p^{\text{H,hydr}}$ ($K_p^{\text{L,elec}} = 500 \text{ L kg}^{-1}$, $K_p^{\text{H,hydr}} = 150 \text{ L kg}^{-1}$ and $C_{s,\text{elec}}^{\text{max}} = 1800 \mu\text{g kg}^{-1}$) and case 2 is when $K_p^{\text{L,elec}} < K_p^{\text{H,hydr}}$ ($K_p^{\text{L,elec}} = 100 \text{ L kg}^{-1}$, $K_p^{\text{H,hydr}} = 150 \text{ L kg}^{-1}$, and $C_{s,\text{elec}}^{\text{max}} = 500 \mu\text{g kg}^{-1}$). C_s^{elec} is divided into a non-labile and labile part above and below the C_w where $K_p^{\text{L,elec}} = K_p^{\text{H,hydr}}$ respectively (if present). The mass concentrations present after the first washing only which reduces C_w from 12 to $6 \mu\text{g L}^{-1}$ are given by entry 6*

$C_w (\mu\text{g L}^{-1})$	$C_s^{\text{total}} (\mu\text{g kg}^{-1})$	$C_s^{\text{hydr}} (\mu\text{g kg}^{-1})$	$C_s^{\text{elec}} (\text{non-labile}) (\mu\text{g kg}^{-1})$	$C_s^{\text{elec}} (\text{labile}) (\mu\text{g kg}^{-1})$
Case 1				
12	2900	1700	600	600
6*	1800	1200	600	0
6	1800	800	600	400
1	600	200	400	0
Case 2				
1	300	200	0	100
6	1100	800	0	300
12	2100	1700	0	400

fraction that is removed is the non-polar adsorbed fraction followed by the stronger bound ionic-polar adsorbed one.

To visualize the different sorption processes Table 7 is derived from Fig. 6 indicating the mass adsorbed by the linear (non-polar) fraction and the labile and non-labile fraction from the non-linear ionic-polar isotherm.

In the following, two desorption processes are distinguished, in Section 3.4.2 a continuous one and in Section 3.4.3 a successive washing one from a complex adsorbent (*e.g.* an adsorbent where either two or more types of sorption processes may occur or that exists out of two or more different types of pure sorbent materials).

3.4.2 A continuous desorption process from a complex adsorbent. In a *continuous desorption* process in case 1 (see Fig. 6) (for example starting from $C_w = 12 \mu\text{g L}^{-1}$) according to the IM model, the first fraction that is removed from the system is the $566 \mu\text{g}$ of the weakest bound, the labile fraction adsorbed by the head until $K_p^{\text{L}} = K_p^{\text{H}}$. Then the complete adsorbed non-

polar fraction ($1800 \mu\text{g}$) is removed and the last fraction is the $818 \mu\text{g}$ of the remaining strongly bound ionic-polar fraction of the surfactant to the sediment. Thus in case 1 three desorption fractions can be observed of which the first and last one are non-linear in character. In case 2 the first fraction that will be removed in a continuous desorption experiment is the $353 \mu\text{g}$ of the labile (ionic-polar) fraction followed only by the $1800 \mu\text{g}$ of the larger and linear fraction of the non-polar interaction. Therefore in case 2 an important difference can be observed between an adsorption and desorption experiment within the IM model. In the adsorption experiment only a linear adsorption process is observed. However if one would follow this adsorption experiment by a desorption one, two fractions will be observed: a first fast but usually small non-linear one from the weaker interaction of the substance with the second fraction(s) in the sediment followed by a larger but linear desorption process from the main linear isotherm. Such mixed rate desorption rate behaviour of non-polar substrates has been

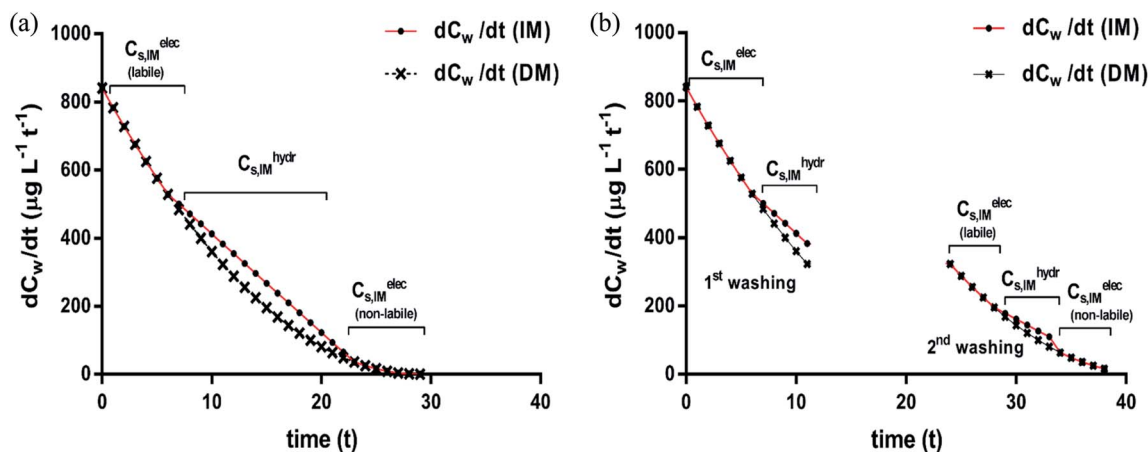


Fig. 7 Desorption rates after a single continuous washing (a) and two successive washings (b); desorption rate curves according to the DM (×) and IM (●) model applied to case 1 in Fig. 6. The subsequent desorption fractions from the two sorption isotherms (non-polar and ionic-polar) according to the IM model are indicated. Note the different slope ranges that coincide with changes of desorption processes for the IM model and note that the adsorbed ionic-polar fraction is divided into a labile and non-labile one. The C_w where this change occurs is the C_w where $K_p^{\text{L,elec}} = K_p^{\text{H,hydr}}$.



observed several times when SOM was used as adsorbents *e.g.* ref. 53 and 54. However authors have not observed a similar behaviour for surfactants. This desorption behaviour is completely different in the DM model since the overall sorption process is only described by a single Langmuir isotherm and desorption in this case is then expected to be only non-linear. The difference in rate constants between the two models is depicted in Fig. 7a.

3.4.3 A successive washing desorption process from a complex adsorbent. In the case of *successive washing* an additional feature of the IM model can be found. If the first washing removes the labile fraction and maybe a small part of the non-polar fraction, then at the end of the first washing period the system is not in equilibrium anymore. This can be visualized by considering that *e.g.* the first washing process diminishes C_w from $12 \mu\text{g L}^{-1}$ to $6 \mu\text{g L}^{-1}$ for case 1 (Table 7). In this case in total $1160 \mu\text{g}$ has been washed off. The first $566 \mu\text{g}$ originates from the desorption of the labile (weakest) ionic-polar bonded fraction and the additional $594 \mu\text{g}$ from the non-polar fraction. At the end of the first washing $1384 - 566 = 818 \mu\text{g}$ is still adsorbed by the ionic-polar interaction and $1800 - 594 = 1206 \mu\text{g}$ by the non-polar interaction. However as can be seen in Table 7 for the equilibrium sorption values at $C_w = 6 \mu\text{g L}^{-1}$ ($1125 \mu\text{g}$ adsorbed by the ionic-polar interaction and $900 \mu\text{g}$ adsorbed by the non-polar interaction) the system is not in equilibrium anymore after the first washing. If the time between each successive washing is sufficient to re-establish equilibrium a small surfactant flux of $307 \mu\text{g}$ adsorbed by the non-polar interaction (the tail) will desorb and flow to the labile adsorption places where it will adsorb by a ionic-polar interaction (the head) to the sediment until a new equilibrium has been established. In the next washing this labile fraction will desorb again. If the driving force of this new flow rate is diffusion only then it may take a long time before this new equilibrium is achieved. The different rate curves for case 1 are depicted in Fig. 7b. The same process can repeat itself until the amount of mass is not sufficient anymore to establish a sufficient mass flow. Contrary to the DM model the IM model is not in equilibrium anymore after any action of dilution.

On similar grounds the fraction that is removed in case of case 2 is $980 \mu\text{g}$ of which $373 \mu\text{g}$ is from the complete labile bound ionic-polar fraction and an additional $637 \mu\text{g}$ from non-polar fraction. If the time between the washing process is sufficient to re-establish equilibrium a small surfactant flux of $273 \mu\text{g}$ adsorbed by a non-polar interaction will desorb and flow to the labile ionic-polar adsorbent.

We conclude here that only the IM model can lead to mixed rate desorption isotherms of first and second order processes when different sediment fractions are involved in the sorption process of the adsorbate while for the DM model only second order processes should be observed. After a washing process the IM model predicts also a mass flow of the surfactant to other adsorbents without invoking any additional physical and/or chemical process of the adsorbate or adsorbent itself.

3.4.4 Hysteresis phenomena. If equilibrium is not achieved after the first washing of case 2 a higher fraction will remain bound to the non-polar adsorbent and a smaller part to the labile ionic-polar adsorbent. In the next washing within the same time span less material will be desorbed than expected. Differences in adsorbed and desorbed fractions are known as hysteresis usually distinguished between pseudo- or kinetic hysteresis and irreversibility where additional chemical and/or physical processes to the adsorbed substance may have occurred. To this end the hysteresis index, HI,^{55–57} was developed which can also be a function of time, t , apart from the temperature, T , and C_w . According to the IM model HI values are larger on increasing C_w since the non-linear isotherm indicates a lower $K_p(C_w)$ and therefore weaker bound fractions at higher C_w . However the adsorbent is stronger bound at lower concentrations and in the same time span, on the condition that equilibrium has not been reached after each washing, smaller fractions will desorb. This part of hysteresis, exemplified above, is normally called kinetic hysteresis contrary to irreversibility where the adsorbed substance and/or adsorbent may have undergone additional processes in a second stage.^{23,58} However at low concentrations this difference may be difficult to distinguish since depending on the experimental conditions one may need to distinguish between the time to reach equilibrium when diffusion is the rate limiting step or when additional processes of the adsorbent or adsorbate occurs.

3.5 Both non-polar and ionic-polar Langmuir isotherms: K_{oc} and f_{oc} vs. K_L^{hydr} and $C_{s,hydr}^{max}$

Experiments where the non-polar interaction has been described by a Langmuir isotherm do exist but most authors do not relate the different sorption parameters K_{oc} and f_{oc} to K_L^{hydr} and $C_{s,hydr}^{max}$. One example is the sorption experiment of the cationic surfactant dodecylpyridinium (DP) onto sediment “EPA12”⁵⁹ where a multisite competitive Langmuir model was developed to explain the sorption behaviour. In this model each site was characterized by a constant K_p^L and a specific value of C_s^{max} . However by invoking a varying K_p^L ($K_p^L(C_w)$) and a unique value of C_s^{max} for both defined interactions (ionic-polar and non-polar), this multisite competitive model changes into a much simpler model of two Langmuir isotherms according to the IM model. In this case, $C_{s,hydr}^{max}$ for the non-polar interaction of DP with the sediment “EPA12” was found to be $\sim 75 \text{ mmol}$ ($\sim 25\,000 \text{ mg}$) dodecylpyridinium per kg sediment. This corresponds to a maximum sediment sorption capacity of around 2.5% (m/m) for DP, which is coincidentally similar to the organic carbon fraction of this sediment (2.1–2.3%).

Sorption experiments of phenanthrene to marine sediment⁶⁰ were described by several isotherms including Langmuir. Using the reported Langmuir data and assuming that only non-polar sorption occurs the data shows the expected linear correlation between $C_{s,hydr}^{max}$ (mmol kg^{-1}) and f_{oc} (%), leading to $C_{s,hydr}^{max} = 0.68f_{oc} + 0.10$ ($N = 5$, $R^2 = 0.88$) and an average $K_L^{hydr} = 316 \text{ L mmol}^{-1}$ or $K_{oc} = 30\,400 \text{ L kg}^{-1}$ (see Table S2†). Using the linear correlation a value of $C_{s,hydr}^{max}$ (mmol kg^{-1}) of 1.7 mmol kg^{-1} sediment for $\sim 2.2\%$ oc is found. Whether this difference in



$C_{s,hydr}^{max}$ between phenanthrene (1.7 mmol kg^{-1} sediment) and DP (75 mmol kg^{-1} sediment) for the same fraction of oc of 2.2% is caused by a different type of organic carbon or by a difference in size of the molecules or both remains to be investigated. We conclude here that relating K_{oc} values to K_L^{hydr} ones is only possible if the ratio of f_{oc} to $C_{s,hydr}^{max}$ is known. This can only be obtained if complete non-polar Langmuir adsorption isotherms are established until the saturating plateau. It is as yet unknown if this ratio depends on the type of organic carbon or is a purely constant one. However in the case of non-polar sorption only it has been reported that the ratio seems to be constant but that the intercept varies which was attributed to different adsorption processes to two types of organic carbon.⁶¹

4. Validation and implications

4.1 Independent-mode or dual-mode

Although the DM model is attractive due to its simple overall standard free enthalpy equation (see Table 2), we have shown that many sorption experiments of surfactants at environmentally relevant concentrations can be interpreted correctly by the IM model only. The Virial applied to LAS⁵ and the NICA-Donnan model applied to PFCA¹¹ were developed to interpret an additional non-polar sorption process (Virial) or ionic-polar sorption process (NICA-Donnan). These models include the additional sorption process by an addition of the different standard free enthalpies, indicating a direct influence of the sorption strength of the head by the tail or *vice versa*. Table 2 shows that this corresponds to the DM model.

Evaluation reveals that these two models are used in cases where a specific sorption process dominates. However if the perturbation (δ) remains small compared to the main sorption process, e.g. $\Delta_s G_{hydr}^0 \gg \Delta_s G_{elec}^0$, then it can be easily derived that $\Delta_s G_{total}^0(IM)$ (Table 2) will lead to an equivalent expression of $\Delta_s G_{total}^0(DM)$ since $\ln(1 + \delta) \approx \delta$. In that case $\Delta_s G_{total}^0(IM) = (\Delta_s G_{main}^0 + \delta \Delta_s G_{per})$ will become equal to $\Delta_s G_{total}^0(IM) = \Delta_s G_{hydr}^0 + \delta \Delta_s G_{elec}^0$ which is exactly the standard free enthalpy expression for the DM model applied in the NICA-Donnan model. A similar expression can be developed when the main adsorption process is ionic-polar in character, the basis of the Virial model and was also shown before in Fig. 2a for case 0 and 1. Consequently the defined Virial K is equal to $K_{p,0}^{total}$ in the DM model (Table 2). Although mathematically $\Delta_s G_{total}^0(IM)$ will become equivalent to $\Delta_s G_{total}^0(DM)$ when accounting for a small perturbation of the main sorption process, the physical picture of individual molecules of surfactants adsorbed only to different sediment fractions has not changed. The Virial and NICA-Donnan models fail to describe the sorption isotherm correctly when the other process becomes more dominant, e.g. by increasing the organic carbon fraction in case of the Virial. It implies that when conducting sorption experiments at low surfactant concentrations with complex adsorbents (like sediment, soil, or even clay), one needs to consider which specific adsorbents are involved in the adsorption processes, and describe each adsorption process independently by a Langmuir isotherm. The experimentally applied system boundaries determine if the specific Langmuir isotherm will appear as a linear one or as a Langmuir one (see

Section 2.2.1). In river sediments and soils the non-polar adsorbent fraction is most likely much larger than the ionic-polar one, while in sea sediments this might be the opposite. Under these conditions (one fraction much larger than the other) the overall adsorption process can often best be described by a linear term and a Langmuir one, and the desorption rate processes will show a mixed character of linear and non-linear rate constants. We note here that the same characteristics are also observed with the polar substance estrone⁶² and non-polar substances in general adsorbed to Sediment Organic Matter (SOM). Our sorption expressions return in the Dual-Mode (DM-SOM),²⁹ the Distributed Reactivity Model (DRM)⁶³ and the OM-clay model applied for non-ionic surfactants sorbing to marine sediment.⁴⁸ However the interpretation of the observed values in the DM-SOM and DRM model differs with the IM model. In the IM model the linear and non-linear contributions are described by simple Langmuir adsorption isotherms related to different adsorbents, respectively. In the DM-SOM model a so-called dissolution domain, leading to a linear term is distinguished from hole-filling domains contributing to the non-linear terms. In the DRM model for natural systems, composite isotherm behaviour is considered as the resultant of a series of near-linear absorption reactions and nonlinear adsorption reactions. The IM model supports the statement that usually one linear term and one or two Langmuir terms are required to obtain "best-fit" models^{64,65} that describe the sorption to SOM. Finally one should realize that better statistics of one model compared to the other do not necessarily imply that the former should be selected, because the error in the measurements themselves are often not taken into consideration.

4.2 The cause of the increase of K_L for ionic-polar or non-polar adsorption when varying the surfactant tail length

The observation that the K_L increases and therefore its corresponding $\Delta_s G^0$ decreases with a constant value when the tail-length of the surfactant increases with one CX_2 -unit is an important aspect in sorption models and SARs. The constant decrease of the free enthalpy of adsorption of surfactants to gaseous films has been known as Traube's rule. According to Aranow,⁶⁶ the constant contribution in the free enthalpy of adsorption ($\Delta \Delta_s G_L^0$) was attributed to an increase of an entropy ($\Delta \Delta_s S_L^0$) rather than a decrease in enthalpy ($\Delta \Delta_s H_L^0$). Aranow attributed this increase of the entropy to an increase of energy levels caused by an increase of torsional oscillators of the additional CH_2 -group in air.

Modern views on the entropy contribution are related to the decrease of the rotational and/or translational movements of the water molecules in the shell around the non-polar tail of the surfactant molecule. Two models attempt to explain this source of entropy loss, the clathrate cage model and the scaled particle cavity model.^{67,68} The loss of entropy is released when the surfactant is adsorbed to the sorbent. Compared to the complete release of the surfactant molecule from the bulk water phase, the entropy increase is expected to be less when an ionic-polar adsorption process prevails, because the tail still remains (partially) in the water-sorbent interface. In the case of a non-polar adsorption process the tail is adsorbed to the adsorbent



out of the water interface leading to a higher free enthalpy release ($\Delta_s G_{L,hydr}^0 > \Delta_s G_{L,elec}^0$) and a higher value of the slope ($\Delta\Delta_s G_{L,hydr}^0 > \Delta\Delta_s G_{L,elec}^0$) is expected. In other words the main contribution factor to a decrease of the standard free enthalpy of adsorption ($\Delta\Delta_s G_L^0 < 0$) when the tail length of *e.g.* a PFCA increases, is a relatively large increase in entropy release of the molecular system ($\Delta\Delta_s S_{L,CF_2}^{0,CF_2} \gg 0$). This causes an increase in the Langmuir sorption constant K_L , and not an extra enthalpy term ($\Delta\Delta_s H_{L,CF_2}^{0,CF_2}$) like an additional interaction of the tail with the sorbent. However, the difference in increment is different for each type of interaction (ionic-polar and non-polar).

4.3 Sorption processes in environmental risk assessment models

The IM model can also describe observed sorption phenomena for surfactants adequately in any ERA model. Basically both types of interaction, non-polar and ionic-polar, are described by a Langmuir isotherm of the specific sediment fraction. However in an ERA model the systems considered (catchment, country) are usually quite large and thus the linear approach (*cf.* eqn (3a) and (3b)) is valid. When estimating the partition coefficient for an unknown surfactant one faces the problem that two parameters must be estimated for each adsorbent: K_L and C_s^{\max} . The value of K_L can be estimated from SARs. However the problem to estimate C_s^{\max} remains, reason why simple sediment parameters are looked for. This concept has only been applied extensively to the non-polar interactions and many SARs have been developed to estimate the K_{oc} of a specific chemical⁶⁹ based on the organic carbon fraction of the sediment, f_{oc} , as a substitute of $C_{s,hydr}^{\max}$.

For the development of estimation methods for the ionic-polar interaction of the surfactant their corresponding K_L^{elec} and C_s^{\max} or their related K_{norm}^{elec} and f_{sed} must be established. These estimation methods are hardly known due to several reasons. Firstly, several types of ionic-polar interactions are known *e.g.* cationic, anionic, non-ionic and zwitter-ionic. For each of these types it may be required to set up a separate K_{norm}^{elec} estimation system. Secondly, before any estimation model can be developed a set of proper K_{norm}^{elec} data must be established. These steps are lacking in the development of a sorption SAR for anionic surfactants.³⁵ In this case the infinite dilution sorption values, correctly obtained as a first step, were not separated into their corresponding sorption processes as they should have been (see Table 2) and any possible salt effect and therefore K_p could not be corrected for the system parameter, C_s^{\max} , for the separate sorption processes. Consequently in the established SAR the use of f_{oc} or CEC (Cation Exchange Capacity) descriptors as independent parameters (eqn (8) and (9) in ref. 35) reflects only the variation in C_s^{\max} *cf.* eqn (3), and the use of the CMC descriptor only considers a non-polar interaction parameter for the specific sorption process of the selected anionic surfactants, even though it is expected that also ionic-polar adsorption will occur.

Simple sediment parameters that estimate C_s^{\max} for the different types of surfactants have not been established well. Depending of the type of interaction three types of sediment parameters are found in the literature that are related to

C_s^{\max} ; (a) parameters directly related to C_s^{\max} (*e.g.* the CEC for cationic surfactants)^{30,59,70,71} or the Anionic Exchange Capacity (AEC) for anionic surfactants *e.g.* the difference in sorption capacity of PFCAs on the anionic exchangers WAX and MAX,⁵¹ (b) the specific surface area (SSA) of the sediment sorption system^{48,72} for non-ionic surfactants or (c) specific sediment parameters *e.g.* oc content or Fe/Al, Si/Al or Fe + Al/Si ratio^{49,50,73–76} for anionic surfactants. Currently the CEC seems to be the only sediment parameter that gives a reasonable direct correlation with $C_{s,cat}^{\max}$. The SSA can only be used when a single sorbent is present. In that case it can relate the adsorbed mass to the surface coverage, very useful in understanding the molecular sorption process. However if different sorbents are present that are both interacting in the sorption process each with a different C_s^{\max} , the SSA is only an overall sediment parameter that cannot be related to one or both of the required C_s^{\max} . Structural sediment parameters like f_{oc} of Fe/Al ratio have the disadvantage that their exact relationship to C_s^{\max} is unknown but are very useful to develop estimation methods for normalised sorption coefficients.

4.4 Possible formation of micellar structures

Sorption of some surfactants at higher concentrations may result into the formation of micellar structures at the surface of the adsorbent (hemi-micelles and/or admicelles) as is well known on pure surfaces (*e.g.* LAS).^{1,3} It is generally assumed that the surface is then fully covered by one layer of surfactant leading to an additional non-polar adsorption process by the tail until twice the C_s^{\max} values. However when sediment is used as adsorbent this is not observed each time, see *e.g.* Section 3.3.2. From a thermodynamic point of view these micellar structures will not be formed when the sorption isotherm can be represented by eqn (4) ($V_{syst} \approx V_L$) and at $C_w(aq) = CMC$ the value of C_s^{\max}/CMC ($L\ kg^{-1}$) is (much) smaller than the minimum aggregation number required to form a micelle at the CMC. For C_s^{\max} of $\sim 8600\ mg\ L^{-1}$, as observed in the experiments of Istok *et al.*,²⁶ the ratio of C_s^{\max}/CMC for LAS₁₀ (1989/500) and LAS₁₂ (2770/125) is ~ 4 and ~ 22 , respectively, which falls still far from the minimum aggregation number at the CMC for these two LAS-compounds, 56 and 68 respectively.⁷⁷ Consequently no micellar structures at the surface of the adsorbent are observed even at these high surfactant concentrations. If the experiment would have been repeated with pure LAS-C₁₀ and LAS-C₁₂, the ratios would have been $\sim 8600/500 = \sim 17$ and $\sim 8600/125 = \sim 70$ respectively. A micellization process of LAS₁₂ could have been expected at the surface of the adsorbent at these high surfactant concentrations.

5. Experimental modifications and final remarks

In this study it has been shown that for sorption to complex adsorbents, such as sediment or soil, at environmentally relevant concentrations the full sorption isotherm of surfactants can be described well by the IM model. When performing such sorption experiments the most relevant adsorbents in the system must be established first. In river sediment and in soils one starts usually



with the organic carbon fraction but adsorbents relevant for the possible ionic-polar interaction are often not well characterized. Once these adsorbents are characterised, the pertaining sorption process at low concentrations can be described by simple Langmuir isotherms. The experimentally applied system boundaries (the volume of the water and the fractions of adsorbents) determine how the Langmuir isotherms will appear at low concentrations. In ERA models it is assumed that these boundaries are so large that every contribution to the overall sorption process can be described by linear contributions. The main issue here is how to establish the sorption constant of the ionic-polar or non-polar adsorption process and the corresponding C_s^{\max} of each adsorbent so that eqn (3a) can be applied. In lab experiments with much smaller system dimensions the C_s^{\max} of one adsorbent may be larger than the one of another sorbent, rendering support to describe the sorption process by a combination of one Langmuir isotherm and a linear contribution or only Langmuir ones. We would like to emphasise here that such a procedure is also applicable to air/soil adsorption processes, adsorption on different types of organic carbon, inorganic sorbents, *etc.* Current ERA models for surfactants underestimate the adsorbed fraction in those cases where the ionic-polar interaction is substantially present, for example in sea sediments or clay-rich sediments or soils.

One needs also to be careful to interpret differences in $K_{p,0}$ when varying a system parameter like pH or ionic strength of the water. According to eqn (3) the $K_{p,0}$ is a product of K_L and C_s^{\max} . Consequently the influence of the variation on both parameters must be established. For example an increase in the Virial partition coefficient upon addition of calcium ions has been observed.⁵ If $[Ca^{2+}]$ (or any other experimental parameter, *e.g.* pH) is varied, the complete isotherm must be established again to derive the relevant parameters, $K_{p,0}^{L, \text{Virial}}$ or K_L and b or C_s^{\max} . If the full Virial isotherm had been established in this case then the increase of $K_{p,0}^{L, \text{Virial}}$ could have been related either to an increase in K_L (and the increase in the partition coefficient $K_{p,0}^{L, \text{Virial}}$ is caused by an increase in the sorption strength of the surfactant molecules onto the sediment), or to an increase in C_s^{\max} (*cf.* eqn (3)) (and the increase in the partition coefficient $K_{p,0}^{L, \text{Virial}}$ is caused by an increase in the number of sorption locations). In case the increase in the partition coefficient $K_{p,0}^{L, \text{Virial}}$ is caused by an increase in C_s^{\max} , an equivalent increase in the capacitance ' b ' at low concentrations (eqn (6)) would also have been measured. Even this incorrect sorption model can result in a correct interpretation because, as explained in Section 4.1, such types of sorption isotherms can be observed if the non-polar adsorption constant is much smaller than of the ionic-polar one.

For modelling purposes and SAR development a variation of the tail length of the surfactant is an important molecular property.⁵² It is well known that the molecular sorption constant always increases for both an ionic-polar and non-polar sorption process of a surfactant when increasing the tail length. This incremental value is different for the two different adsorption processes. The most likely cause of these observations is an entropy effect rather than an enthalpy effect caused by the water molecules surrounding the tail of the surfactant.

When interpreting a variation in K_p at a specific C_w due to varying a system parameter (*e.g.* the fraction of sediment) the resulting *exact* K_p values must be compared to each other instead of using the average one. In case of a non-linear isotherm the average K_p leads to a different $K_{p,0}$ at each C_w . This would imply that the (molecular) sorption coefficient, *e.g.* K_L in case of a Langmuir isotherm, differs at each C_w which is obviously incorrect in this case. However the exact K_p at a specific C_w can only be determined if a fitted sorption isotherm has been established through the measured data points. By calculating the exact K_p value at a specific C_w one may observe whether the exact K_p increases or decreases when varying the sediment fraction (see also Annex I). The IM model can also well explain a number of different desorption phenomena in sediment or soil. IM can define labile and non-labile desorption fractions from the same Langmuir isotherm. IM also shows that in successive washings, material flows from one adsorbent to other ones will occur because the system is forced out of equilibrium. We also showed that if one applies a Langmuir isotherm and a linear one for the different adsorbents, second order and first order desorption rates can be observed. While this has been observed for non-polar substances already, in the literature we could not find such phenomena for surfactants.

The IM model is most likely the best model to describe sorption on sediment and soil for surfactants at low concentrations. Applying the Freundlich isotherm in environmental chemistry, as is often done, needs to be avoided since the Freundlich model fails for example to derive $K_{p,0}$ relevant for the development of sorption models, nor can it properly describe the environmentally important dilution process. The Freundlich model also does not add to the understanding of the adsorption mechanism of the surfactant or any other substance on the relevant adsorbent.

Annex I

Sorption including sediment fraction as variable parameter

In a typical sorption experiment an amount of sediment, m_s (kg) is added to a specific volume of water, V_L (L) containing an amount of sorbate. The total volume of the experimental system, V_{sys} , is then given by $V_L + \rho m_s$ where ρ is the specific volume ($L \text{ kg}^{-1}$) of the sediment and m_s the mass of the sediment. After the experiment an amount of substance, m_x (mg), is adsorbed to the sediment while an amount, m_{aq} (mg), remains dissolved. The thermodynamic particulate matter concentration, C_s^{therm} , is given by m_x (mg substance)/ m_s (kg sediment) and the dissolved concentration in the experimental system, C_w^{sys} , by m_{aq}/V_L ,⁷⁸ where m_{aq}/V_L is the thermodynamic dissolved concentration, C_w^{therm} . The experimental Langmuir case I sorption isotherm is then given by (A1)

$$\frac{m_x}{m_s} = \frac{K_{p,0}^L \frac{m_x^{\max}}{m_s} \frac{m_{\text{aq}}}{V_L} \frac{V_L}{V_{\text{sys}}}}{\frac{m_x^{\max}}{m_s} + K_{p,0}^L \frac{m_{\text{aq}}}{V_L} \frac{V_L}{V_{\text{sys}}}} \quad (\text{A1})$$



where m_x^{\max} is the maximum sorption capacity of the applied sediment. For convenience the amount of the sediment present in the system, m_s , is set as the fraction, f_s (m_s kg dry sediment/ M_s kg dry sediment) multiplied by M_s (kg dry sediment), the mass normalization factor. Eqn (A1) can be rearranged into eqn (A2), the thermodynamic form in several ways depending on the type of experimental parameter reported

$$C_s^{\text{therm}} = \frac{m_x}{M_s} = \frac{K_{p,0}^L \frac{m_x^{\max}}{M_s} C_w^{\text{therm}} \frac{f_s V_L}{V_L + \rho f_s M_s}}{\frac{m_x^{\max}}{M_s} + K_{p,0}^L C_w^{\text{therm}} \frac{f_s V_L}{V_L + \rho f_s M_s}} \\ = \frac{K_{p,0}^L C_s^{\max} C_w^{\text{therm}} \frac{f_s}{1 + \rho S_{\text{aq}}}}{C_s^{\max} + K_{p,0}^L C_w^{\text{therm}} \frac{f_s}{1 + \rho S_{\text{aq}}}} \quad (\text{A2})$$

where S_{aq} (kg sediment per L water) is the sediment concentration in the applied experimental system. Eqn (A2) includes all the different sorption isotherms and assumptions but has the disadvantage that both the sediment fraction, f_s , and the selected mass normalisation, M_s , or the sediment concentration in the water, S_{aq} , are included. The following assumptions lead to different sorption equations:

(1) In case $\rho f_s M_s \ll V_L$ ($V_{\text{sys}} \approx V_L$) or $\rho[S]_{\text{aq}} \ll 1$ and sorption is normalised to 1 kg of sediment ($f_s = 1 \text{ kg kg}^{-1}$, $M_s = 1 \text{ kg}$), eqn (A2) is approximated by eqn (A3), the thermodynamic Langmuir sorption isotherm necessary to derive the proper sorption constant $K_{p,0}^L$

$$C_s^{\text{therm}} = \frac{K_{p,0}^L C_s^{\max} C_w^{\text{therm}}}{C_s^{\max} + K_{p,0}^L C_w^{\text{therm}}} \quad (\text{A3})$$

Eqn (A3) is normally used in a typical sorption experiment where a small amount of sediment is mixed with a relatively large and constant amount of water with varying mass of surfactant and the data are normalised to 1 kg of sediment and 1 L of water.

(2) In case M_s and V_L are normalised to 1 kg of sediment and 1 L respectively and in addition $C_w^{\text{therm}} = \text{constant}$, then eqn (A2) turns into eqn (A4),

$$C_s^{\text{therm}} = \frac{K_{p,0}^L C_s^{\max} C_{w,\text{const}}^{\text{therm}} \left(\frac{f_s}{1 + \rho f_s} \right)}{C_s^{\max} + K_{p,0}^L C_{w,\text{const}}^{\text{therm}} \left(\frac{f_s}{1 + \rho f_s} \right)} \\ = \frac{K_{p,0}^L C_s^{\max} C_{w,\text{const}}^{\text{therm}} \frac{f_s}{1 + \rho S_{\text{aq}}}}{C_s^{\max} + K_{p,0}^L C_{w,\text{const}}^{\text{therm}} \frac{f_s}{1 + \rho S_{\text{aq}}}} \quad (\text{A4})$$

Eqn (A4) shows the variation of the C_s^{therm} with varying fractions of sediment, f_s (kg kg^{-1}), or sediment concentrations, S_{aq} (kg L^{-1}), present in the system keeping $C_w^{\text{therm}} = \text{constant}$. Experimentally this condition is very difficult to achieve. However by establishing a series of full adsorption isotherms, each with the same total mass of the sorbate but a varying

sediment fraction,^{5,79} one can compare the exact K_p 's at a specific C_w^{therm} .

(3) Eqn (A4) leads also to $C_s \rightarrow K_{p,0}^L C_{w,\text{const}}^{\text{therm}} (f_s/(1 + \rho f_s))$ or $C_s \rightarrow K_{p,0}^L C_{w,\text{const}}^{\text{therm}} (f_s/(1 + \rho S_{\text{aq}}))$ in the limiting condition when $C_s^{\max} \gg K_{p,0}^L C_{w,\text{const}}^{\text{therm}} (f_s/(1 + \rho f_s))$ or $C_s^{\max} \gg K_{p,0}^L C_{w,\text{const}}^{\text{therm}} (f_s/(1 + \rho S_{\text{aq}}))$ indicating an increasing fraction of sediment present in the experimental system. This is equivalent to the Langmuir sorption equation for infinite dilution (eqn (3b) in this paper) but corrected for the difference in system. Since under the experimental conditions ρf_s is often $\ll 1$ or $\rho[S]_{\text{aq}} \ll 1$, $C_s \rightarrow K_{p,0}^L C_{w,\text{const}}^{\text{therm}} f_s$ showing that sorption depends of the sediment fraction while keeping C_w constant. In case C_s^{\max} is very small compared to $K_{p,0}^L C_{w,\text{const}}^{\text{therm}} (f_s/(1 + \rho f_s))$, eqn (A4) leads to $C_s \rightarrow C_s^{\max}$, which is the maximum amount of substance that can be sorbed to the sediment.

(4) The observed increase in sorption strength when the sediment fraction increases is different from the variation in sorption strength of strongly non-polar substances caused by the presence of a third phase in the water sometimes indicated as the classical solid effect. In this case it is observed that the sorption strength decreases on increasing sediment fraction, f_s .

Annex II

Rate equation for Langmuir sorption process

The experimental measured adsorption-desorption rate eqn (A5) is the starting point

$$C_w(t) \xrightleftharpoons[k_1]{k_{-1}} C_s(t) \frac{dC_w}{dt} = k_{-1} C_s(t) - k_1 C_w(t) \quad (\text{A5})$$

The equilibrium constant K_p^L is related to both rate constants, $K_p^L = k_1/k_{-1}$, eqn (A6). However these system rate constants are not equivalent to the molecular adsorption-desorption rate constants since this is a different thermodynamic system. In a non-linear sorption process K_p^L is also a function of $C_w(t)$ including in the infinite limit.

$$\frac{dC_w}{dt} = k_1 \left(\frac{C_s(t)}{K_p^L(t)} - C_w(t) \right) \quad (\text{A6})$$

Eqn (A6) is equivalent on assuming that local molecular sorption process(es) is(are) at equilibrium at each moment ($K_L = c^{\text{st}}$) but the overall system sorption process leading to K_p^L is not. Such type of processes are well known and described in non-equilibrium statistical thermodynamics.⁸⁰

Table 2 gives an expression for the exact K_p^L and for C_s at each C_w for the Langmuir molecular sorption process which is turned into an equivalent but time dependent system one, eqn (A7).

$$K_p^L(t) = \frac{K_{p,0}^L (C_s^{\max})^2}{(C_s^{\max} + K_{p,0}^L C_w(t))^2} \quad C_s(t) = \frac{K_{p,0}^L C_s^{\max} C_w(t)}{C_s^{\max} + K_{p,0}^L C_w(t)} \quad (\text{A7})$$

Using eqn (A7) into (A6) and rearranging leads to the following rate expression for the simple case that molecular



sorption process, K_L , is in equilibrium at each moment but the overall system sorption process is not and when the initial concentration is not too high ($C_w(0) \geq C_s(0)$)

$$\frac{dC_w}{dt} = k_1 \frac{K_{p,0}^L}{C_s^{\max}} C_w^2 = k_1 K_L C_w^2 \quad (\text{A8})$$

Thus sorption rate processes following a Langmuir isotherm are of a simple second order nature in C_w as is overwhelmingly observed, *e.g.* ref. 81 and 82, while it is a more complex one for the Virial isotherm. The Freundlich isotherms fails because the infinite limit value is not defined. It is clear that when $C_s(t)$ does not play a role in eqn (A5) (Henry's law regime), a first order rate process is observed.

List of parameters

Parameter	Unit	Description
$\Delta_s G_{\text{elec}}^0$	J mol ⁻¹	Standard free enthalpy of an electrostatic (ionic-polar) adsorption process
$\Delta_s G_{\text{hydr}}^0$	J mol ⁻¹	Standard free enthalpy of a hydrophobic (non-polar) adsorption process
$\Delta_s G_{\text{total}}^0$	J mol ⁻¹	Total standard free enthalpy of adsorption
AEC	mg or mmol anionic ions per kg sediment	Anion exchange capacity
CEC	mg or mmol cationic ions per kg sediment	Cation exchange capacity
CMC	mmol L ⁻¹	Critical micelle concentration
C_s	mg or mmol substance per kg sediment	Adsorbed mass fraction
$C_{s,\text{elec}}^{\max}$	mg or mmol substance per kg sediment	Maximum sorption capacity for an electrostatic or ionic-polar interaction
$C_{s,\text{hydr}}^{\max}$	mg or mmol substance per kg sediment	Maximum sorption capacity for a hydrophobic or non-polar interaction
$C_{s,\text{Virial}}^{\max}$	mg or mmol substance per kg sediment	Virial maximum sorption capacity
C_s^{\max}	mg or mmol substance per kg sediment	Maximum sorption capacity
C_w	mg L ⁻¹ or mmol L ⁻¹	Dissolved concentration
f_{oc}	kg oc per kg sediment	Fraction organic carbon in sediment
f_{sed}	kg parameter per kg sediment	Fraction of a specific parameter in sediment
IEC	mg or mmol ions per kg sediment	Ionic exchange concentration
$K_{p,0}^H = K_p^H$	L kg ⁻¹	Henry's law sediment-water partition coefficient (at any C_w)
K_F	L ⁿ kg ⁻ⁿ mg ⁻⁽ⁿ⁻¹⁾	Freundlich sorption constant
K_L	L mg ⁻¹ or L mmol ⁻¹	Langmuir sorption constant
$K_{p,0}^{L,\text{elec}}$	L kg ⁻¹	Langmuir sediment-water partition coefficient at infinite dilution for an electrostatic or ionic-polar interaction
$K_{p,0}^{L,\text{hydr}}$	L kg ⁻¹	Langmuir sediment-water partition coefficient at infinite

(Contd.)

Parameter	Unit	Description
K_L^{elec}	L mg ⁻¹ or L mmol ⁻¹	dilution for a hydrophobic or non-polar interaction Electrostatic or ionic-polar Langmuir sorption constant
K_L^{hydr}	L mg ⁻¹ or L mmol ⁻¹	Hydrophobic or non-polar Langmuir sorption constant
K_p^L	L kg ⁻¹	Langmuir sediment-water partition coefficient
$K_{p,0}^L$	L kg ⁻¹	Langmuir sediment-water partition coefficient at infinite dilution
$K_{\text{norm}}^{\text{elec}}$	L kg ⁻¹ parameter	Sediment normalised electrostatic or ionic-polar sediment-water partition coefficient
K_{oc}	L kg ⁻¹ oc	Organic carbon normalised hydrophobic or non-polar sediment-water partition coefficient
K_{ow}	L _{octanol} L _{water} ⁻¹	Octanol-water partition coefficient
K_p	L kg ⁻¹	Sediment-water partition coefficient
$K_{p,0}^{\text{elec-DM}}$	L kg ⁻¹	Electrostatic or ionic-polar sediment-water partition coefficient at infinite dilution according to the Dual-Mode model
$K_{p,0}^{\text{elec-IM}}$	L kg ⁻¹	Electrostatic or ionic-polar sediment-water partition coefficient at infinite dilution according to the Independent-Mode model
$K_{p,0}^{L,\text{Virial}}$	L kg ⁻¹	Langmuir Virial sediment-water partition coefficient at infinite dilution
$K_{p,0}^{\text{total}}$	L kg ⁻¹	Total sediment-water partition coefficient at infinite dilution
K_p^{elec}	L kg ⁻¹	Electrostatic or ionic-polar sediment-water partition coefficient
K_p^F	L kg ⁻¹	Freundlich sediment-water partition coefficient
$K_p^{H,\text{elec}}$	L kg ⁻¹	Henry's law sediment-water partition coefficient for an electrostatic or ionic-polar interaction
$K_p^{H,\text{hydr}}$	L kg ⁻¹	Henry's law sediment-water partition coefficient for a hydrophobic or non-polar interaction
K_p^{hydr}	L kg ⁻¹	Hydrophobic or non-polar sediment-water partition coefficient
K_p^V	L kg ⁻¹	Virial sediment-water partition coefficient

Conflicts of interest

There are no conflicts to declare.



Acknowledgements

Authors would like to thank the valuable input from all four anonymous reviewers in improving the structuring of the manuscript and providing critical suggestions to clarify the terminology.

References

- 1 J. Scaemhorn, R. Schechter and W. Wade, *J. Colloid Interface Sci.*, 1982, **85**, 463–478.
- 2 A. Fan, P. Somasundaran and N. J. Turro, *Langmuir*, 1997, **13**, 506–510.
- 3 R. Atkin, V. S. Craig, E. J. Wanless and S. Biggs, *Adv. Colloid Interface Sci.*, 2003, **103**, 219–304.
- 4 P. Chandar, P. Somasundaran and N. J. Turro, *J. Colloid Interface Sci.*, 1987, **117**, 31–46.
- 5 J. C. Westall, H. Chen, W. Zhang and B. J. Brownawell, *Environ. Sci. Technol.*, 1999, **33**, 3110–3118.
- 6 P. Somasundaran, R. Middleton and K. Viswanathan, Relationship between surfactant structure and adsorption, in *Anonymous*, ACS Publications, 1984.
- 7 Y. Ihara, *J. Appl. Polym. Sci.*, 1992, **44**, 1837–1840.
- 8 F. Xiao, X. Zhang, L. Penn, J. S. Gulliver and M. F. Simcik, *Environ. Sci. Technol.*, 2011, **45**, 10028–10035.
- 9 S. T. Droge and K. Goss, *Environ. Sci. Technol.*, 2013, **47**, 14233–14241.
- 10 R. Zhang and P. Somasundaran, *Adv. Colloid Interface Sci.*, 2006, **123**, 213–229.
- 11 C. P. Higgins and R. G. Luthy, *Environ. Sci. Technol.*, 2007, **41**, 3254–3261.
- 12 S. Droge, *Environ. Sci. Technol.*, 2018, **53**, 760–770.
- 13 N. Timmer and S. Droge, *Environ. Sci. Technol.*, 2017, **51**, 2890–2898.
- 14 S. T. Droge, T. L. Sinnige and J. L. Hermens, *Anal. Chem.*, 2007, **79**, 2885–2891.
- 15 J. J. Haftka, P. Scherpenisse, G. Oetter, G. Hodges, C. V. Eadsforth, M. Kotthoff and J. L. Hermens, *Environ. Toxicol. Chem.*, 2016, **35**, 2173–2181.
- 16 W. J. Weber and W. Huang, *Environ. Sci. Technol.*, 1996, **30**, 881–888.
- 17 B. Xing and J. J. Pignatello, *Environ. Toxicol. Chem.*, 1996, **15**, 1282–1288.
- 18 S. Douven, C. A. Paez and C. J. Gommers, *J. Colloid Interface Sci.*, 2015, **448**, 437–450.
- 19 P. M. Gschwend, *Environmental organic chemistry*, John Wiley & Sons, 2016.
- 20 M. Ishiguro and L. K. Koopal, *Adv. Colloid Interface Sci.*, 2016, **231**, 59–102.
- 21 Z. Xu, J. Cai and B. Pan, *J. Zhejiang Univ., Sci., A*, 2013, **14**, 155–176.
- 22 Y. Chen, J. L. Hermens and S. T. Droge, *Environ. Pollut.*, 2013, **179**, 153–159.
- 23 G. Limousin, J. Gaudet, L. Charlet, S. Szenknect, V. Barthes and M. Krimissa, *Appl. Geochem.*, 2007, **22**, 249–275.
- 24 E. M. Webster, *Environ. Rev.*, 2014, **22**, 430–444.
- 25 I. Langmuir, *J. Am. Chem. Soc.*, 1918, **40**, 1361–1403.
- 26 J. Istok, J. Field, M. Schroth, T. Sawyer and M. Humphrey, *Groundwater*, 1999, **37**, 589–598.
- 27 P. S. Bäuerlein, T. L. Ter Laak, R. C. Hofman-Caris, P. de Voogt and S. T. Droge, *Water Res.*, 2012, **46**, 5009–5018.
- 28 N. Narkis and B. Ben-David, *Water Res.*, 1985, **19**, 815–824.
- 29 B. Xing and J. J. Pignatello, *Environ. Sci. Technol.*, 1997, **31**, 792–799.
- 30 R. T. Podoll, K. C. Irwin and S. Brendlinger, *Environ. Sci. Technol.*, 1987, **21**, 562–568.
- 31 M. L. Cano and P. B. Dorn, *Environ. Toxicol. Chem.*, 1996, **15**, 684–690.
- 32 S. J. Traina, D. C. McAvoy and D. J. Versteeg, *Environ. Sci. Technol.*, 1996, **30**, 1300–1309.
- 33 G. Pan, C. Jia, D. Zhao, C. You, H. Chen and G. Jiang, *Environ. Pollut.*, 2009, **157**, 325–330.
- 34 S. Droge and K. Goss, *Environ. Sci. Technol.*, 2012, **46**, 5894–5901.
- 35 D. M. Di Toro, L. J. Dodge and V. C. Hand, *Environ. Sci. Technol.*, 1990, **24**, 1013–1020.
- 36 R. Chen, Y. Zhang, F. Darabi Sahneh, C. M. Scoglio, W. Wohlleben, A. Haase, N. A. Monteiro-Riviere and J. E. Riviere, *ACS Nano*, 2014, **8**, 9446–9456.
- 37 X. Zhou and X. Zhou, *Chem. Eng. Commun.*, 2014, **201**, 1459–1467.
- 38 P. S. Ghosal and A. K. Gupta, *J. Mol. Liq.*, 2017, **225**, 137–146.
- 39 S. Azizian, S. Eris and L. D. Wilson, *Chem. Phys.*, 2018, **513**, 99–104.
- 40 S. Azizian, *J. Colloid Interface Sci.*, 2004, **276**, 47–52.
- 41 E. Matthijs and H. De Henau, *Tenside Deterg.*, 1985, **22**, 299–304.
- 42 J. Rubio, E. González-Mazo and A. Gómez-Parra, *Mar. Chem.*, 1996, **54**, 171–177.
- 43 M. Garcia, E. Campos, J. Sanchez-Leal and F. Comelles, *Tenside, Surfactants, Deterg.*, 2004, **41**, 235–239.
- 44 J. Marchesi, W. House, G. White, N. Russell and I. Farr, *Colloids Surf.*, 1991, **53**, 63–78.
- 45 C. P. Higgins and R. G. Luthy, *Environ. Sci. Technol.*, 2006, **40**, 7251–7256.
- 46 S. T. Droge and J. L. Hermens, *Environ. Sci. Technol.*, 2007, **41**, 3192–3198.
- 47 W. W. John, G. Bao, W. P. Johnson and T. B. Stauffer, *Environ. Sci. Technol.*, 2000, **34**, 672–679.
- 48 S. T. Droge, L. Yarza-Irusta and J. L. Hermens, *Environ. Sci. Technol.*, 2009, **43**, 5712–5718.
- 49 A. Rico-Rico, A. Temara, T. Behrends and J. L. Hermens, *Environ. Pollut.*, 2009, **157**, 377–383.
- 50 Y. Shen and M. Yen, *Environ. Technol.*, 1999, **20**, 425–430.
- 51 C. Eschauzier, *Perfluoroalkyl acids in drinking water: Sources, fate and removal*, Ph.D. thesis, Universiteit van Amsterdam, 2013.
- 52 P. de Voogt, L. Zurano, P. Serné and J. J. Haftka, *Environ. Chem.*, 2012, **9**, 564–570.
- 53 G. Cornelissen, P. C. van Noort and H. A. J. Govers, *Environ. Toxicol. Chem.*, 1997, **16**, 1351–1357.
- 54 M. D. Johnson, T. M. Keinath and W. J. Weber, *Environ. Sci. Technol.*, 2001, **35**, 1688–1695.



- 55 W. Huang, H. Yu and W. J. Weber Jr, *J. Contam. Hydrol.*, 1998, **31**, 129–148.
- 56 W. J. Weber Jr, W. Huang and H. Yu, *J. Contam. Hydrol.*, 1998, **31**, 149–165.
- 57 E. J. LeBoeuf and W. J. Weber, *Environ. Sci. Technol.*, 2000, **34**, 3632–3640.
- 58 A. T. Kan, G. Fu and M. B. Tomson, *Environ. Sci. Technol.*, 1994, **28**, 859–867.
- 59 B. J. Brownawell, H. Chen, J. M. Collier and J. C. Westall, *Environ. Sci. Technol.*, 1990, **24**, 1234–1241.
- 60 G. Yang and X. Zheng, *Environ. Toxicol. Chem.*, 2010, **29**, 2169–2176.
- 61 P. C. Van Noort, M. T. Jonker and A. A. Koelmans, *Environ. Sci. Technol.*, 2004, **38**, 3305–3309.
- 62 J. Zhang, G. Yang, Q. Li, X. Cao and G. Liu, *Mar. Pollut. Bull.*, 2013, **76**, 220–226.
- 63 W. J. Weber Jr, P. M. McGinley and L. E. Katz, *Environ. Sci. Technol.*, 1992, **26**, 1955–1962.
- 64 W. Huang, T. M. Young, M. A. Schlautman, H. Yu and W. J. Weber, *Environ. Sci. Technol.*, 1997, **31**, 1703–1710.
- 65 G. Xia and W. P. Ball, *Environ. Sci. Technol.*, 1999, **33**, 262–269.
- 66 R. H. Aranow and L. Witten, *J. Chem. Phys.*, 1958, **28**, 405–409.
- 67 T. P. Silverstein, *J. Chem. Educ.*, 1998, **75**, 116.
- 68 D. Chandler, *Nature*, 2005, **437**, 640.
- 69 D. Mackay and R. Boethling, *Handbook of property estimation methods for chemicals: environmental health sciences*, CRC Press, 2000.
- 70 S. Xu and S. A. Boyd, *Environ. Sci. Technol.*, 1995, **29**, 312–320.
- 71 M. J. Brown and D. R. Burris, *Groundwater*, 1996, **34**, 734–744.
- 72 B. Wang, W. Chen, H. Fu, X. Qu, S. Zheng, Z. Xu and D. Zhu, *Carbon*, 2014, **79**, 203–212.
- 73 K. Inoue, K. Kaneko and M. Yoshida, *Soil Sci. Plant Nutr.*, 1978, **24**, 91–102.
- 74 Z. Ou, A. Yediler, Y. He, L. Jia, A. Kettrup and T. Sun, *Chemosphere*, 1996, **32**, 827–839.
- 75 Y. Shen, *Chemosphere*, 2000, **41**, 711–716.
- 76 S. Kang and H. Y. Jeong, *J. Hazard. Mater.*, 2015, **284**, 143–150.
- 77 Z. Li, Q. Gong, L. Luo, L. Zhang, S. Zhao and J. Yu, *J. Dispersion Sci. Technol.*, 2011, **32**, 167–173.
- 78 J. F. Pankow and S. W. McKenzie, *Environ. Sci. Technol.*, 1991, **25**, 2046–2053.
- 79 B. J. Brownawell, H. Chen, W. Zhang and J. C. Westall, *Environ. Sci. Technol.*, 1997, **31**, 1735–1741.
- 80 D. Zubarev, V. Morozov and G. Ropke, *Statistical Mechanics of Nonequilibrium Processes, Volume 1 (See 3527400834): Basic Concepts, Kinetic Theory*, Wiley-VCH, 1996.
- 81 C. K. Yeh and L. C. Lin, *J. Environ. Sci. Health, Part A: Toxic/Hazard. Subst. Environ. Eng.*, 2003, **38**, 1145–1157.
- 82 Z. Du, S. Deng, Y. Bei, Q. Huang, B. Wang, J. Huang and G. Yu, *J. Hazard. Mater.*, 2014, **274**, 443–454.

